TMD factorisation
(a phenomenological introduction)

giuseppe bozzi
University and INFN, Cagliari

Collinear PDF (FF)

Collinear PDF
$f(x)$ depend on:
x = longitudinal-momentum fraction

1-dim imaging

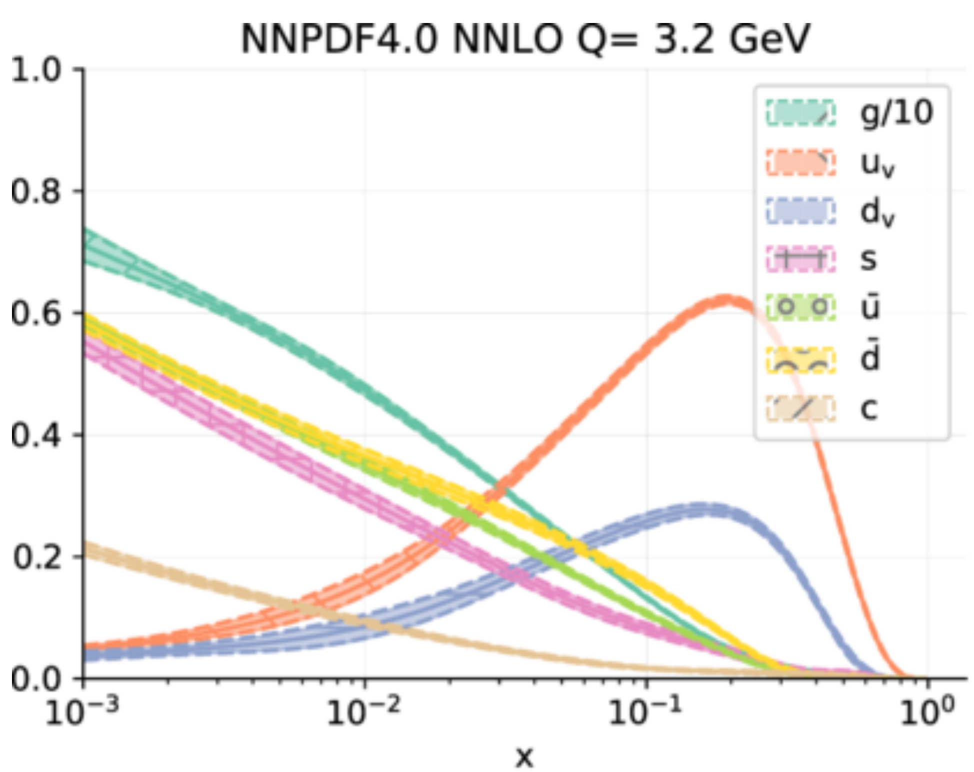

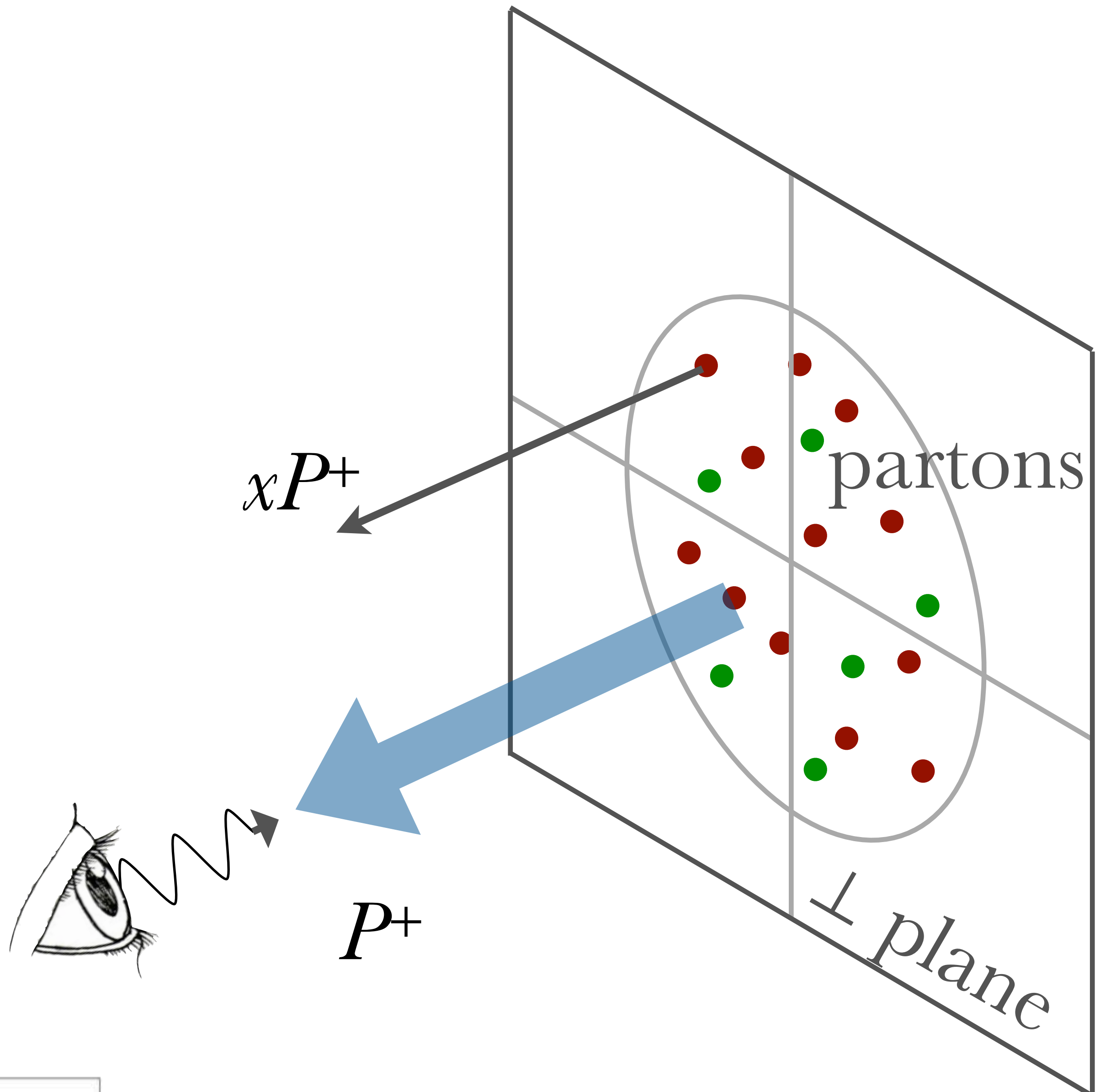

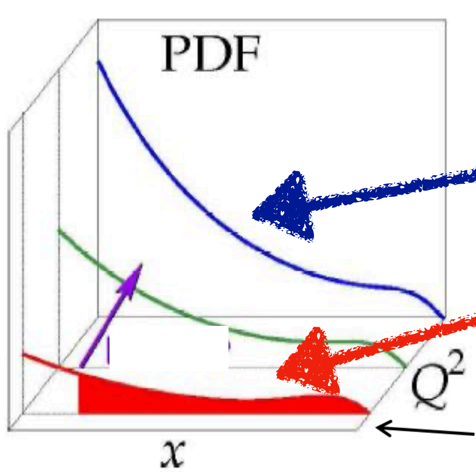

QCD predicts scale evolution

QCD cannot predict x-shape
→PDF fit

TMD PDF (FF)

Transverse **M**omentum **D**ependent **PDF**
$F(x, k_\perp)$ depend on:
x = longitudinal-momentum fraction
$k_\perp$ = *(intrinsic)* transverse-momentum

3-dim imaging

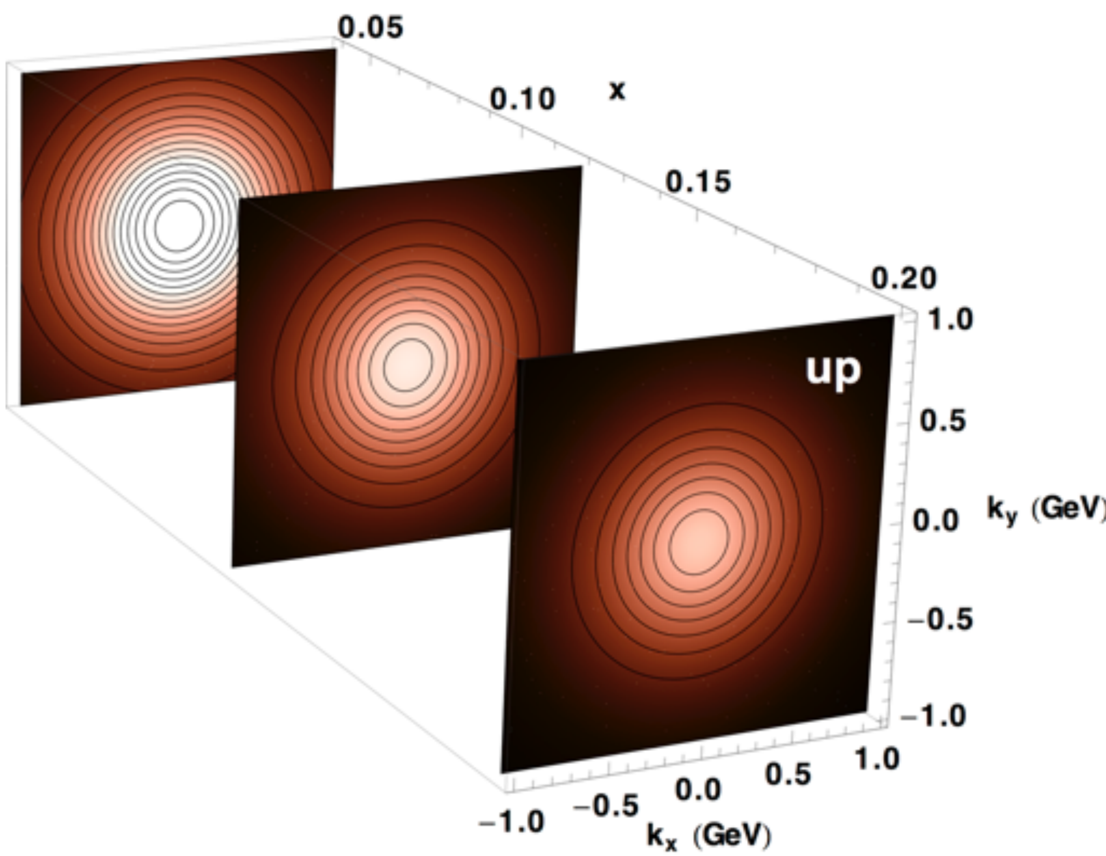

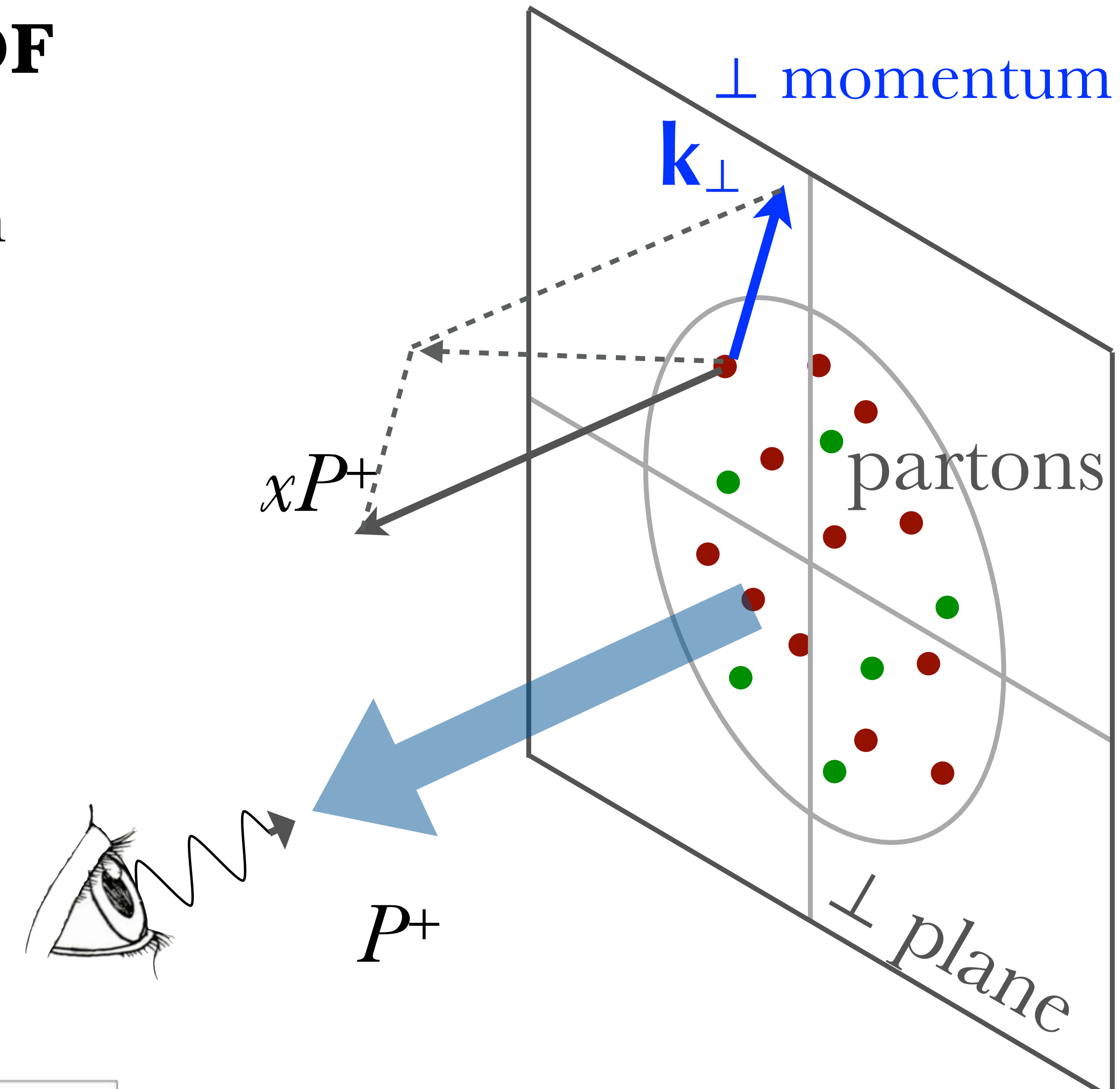

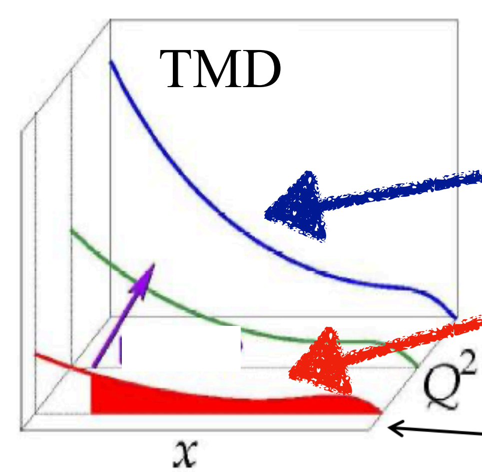

QCD predicts scale evolution

QCD cannot predict $x, k_\perp$-shape
→TMD fit

Factorising processes

- Processes for which TMD factorisation has been **proven**:

Drell-Yan

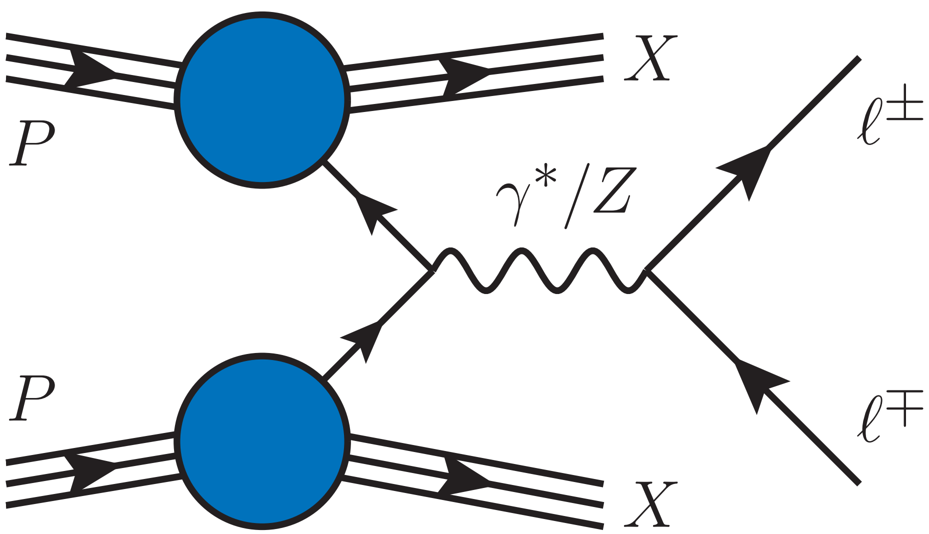

$PP \longrightarrow \ell^\pm \ell^\mp X$

Semi-inclusive DIS

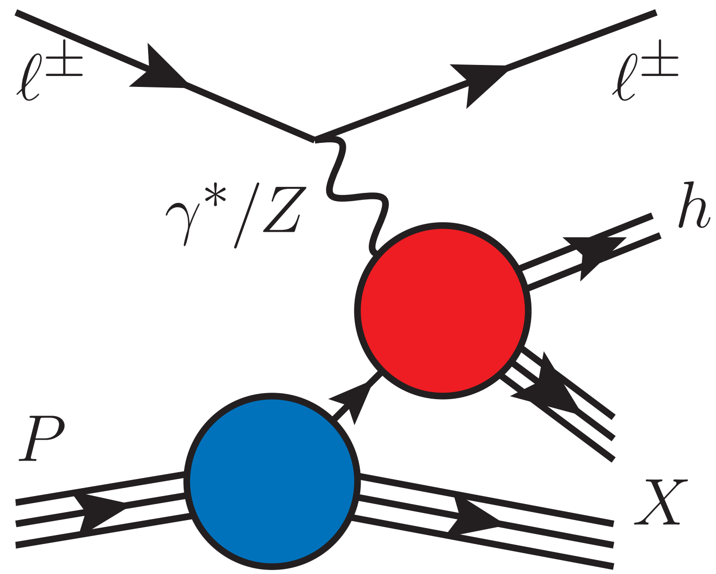

$P\ell^\pm \longrightarrow \ell^\pm h X$

e^+e^- annihilation

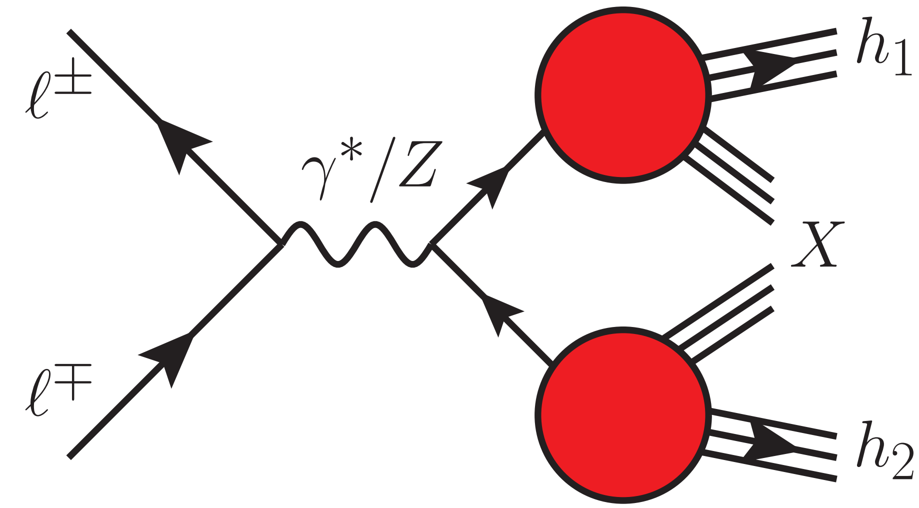

$\ell^\pm \ell^\mp \to h_1 h_2 X$

- **Two** TMD **PDFs**
- Lots of data:
  - low-energy: FNAL
  - mid-energy: RHIC
  - high-energy: Tevatron, LHC

- One TMD **PDF** one **FF**
- many precise data points:
  - HERMES at DESY
  - COMPASS at CERN

- **Two** TMD **FFs**
- DIA process from:
  - BELLE at KEK
  - BABAR at SLAC

missing!

TMD factorisation for DY

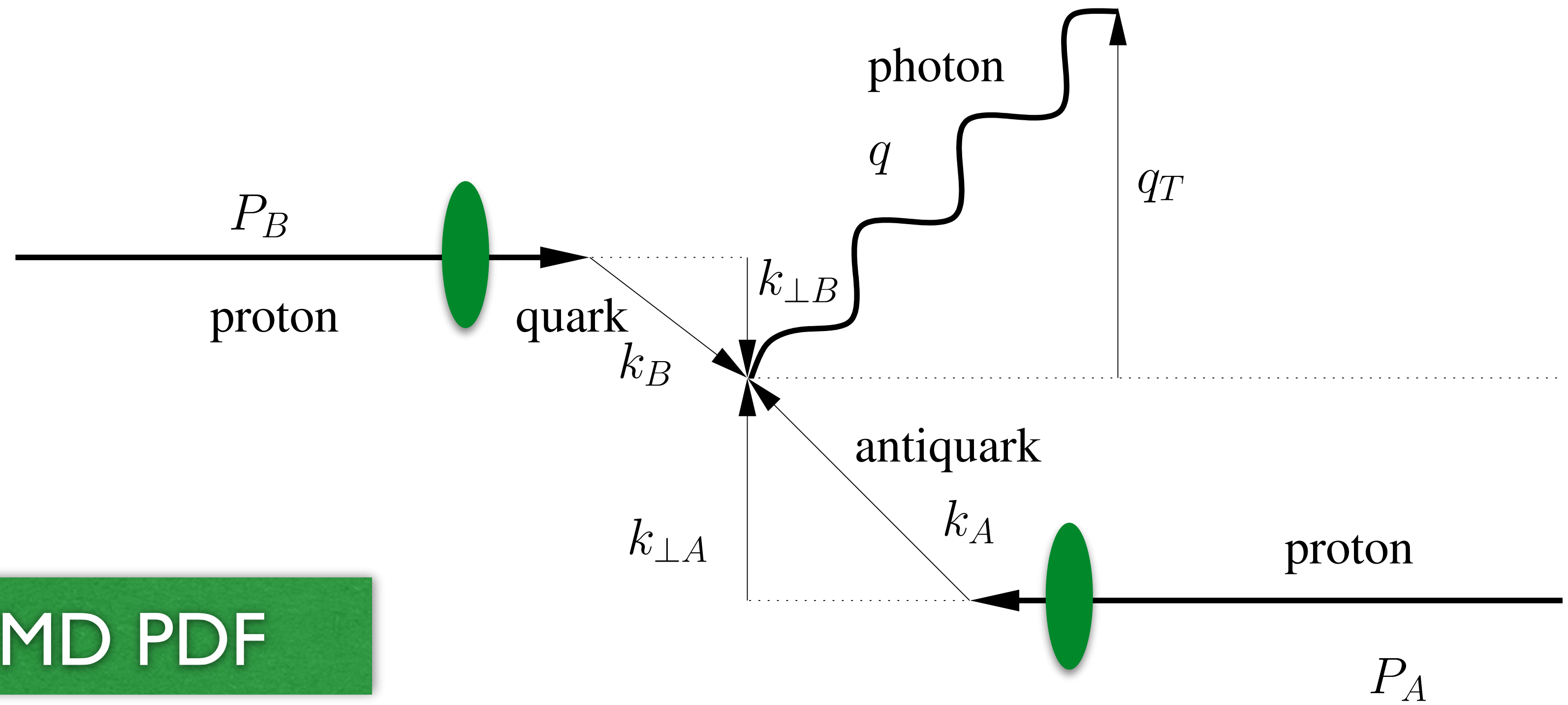

quark TMD PDF

$$\frac{d\sigma}{dq_T\,dy\,dQ} \propto x_A x_B H^{DY}(Q,\mu) \sum_q c_q(Q^2) \int d^2\mathbf{k}_{\perp A}\, d^2\mathbf{k}_{\perp B}\, F^{\bar{q}}(x_A, \mathbf{k}_{\perp A}^2; \mu, \zeta_A)\, F^q(x_B, \mathbf{k}_{\perp B}^2; \mu, \zeta_B)\; \delta^{(2)}(\mathbf{k}_{\perp A} + \mathbf{k}_{\perp B} - \mathbf{q}_T)$$

$$= x_A x_B H^{DY}(Q,\mu) \sum_q c_q(Q^2) \int \frac{db_T}{2\pi}\, b_T\, J_0(b_T q_T)\; \hat{F}^{\bar{q}}(x_A, b_T^2; \mu, \zeta_A)\, \hat{F}^q(x_B, b_T^2; \mu, \zeta_B)$$

TMD factorisation

- TMD factorisation introduces two independent *artificial* scales:
  - the **renormalisation scale** $\boldsymbol{\mu}$, originating from UV renormalisation
  - the **rapidity scale** ζ, originating from the cancellation of rapidity divergencies between collinear and soft emissions

- The respective **evolution equations** are:

$$\frac{\partial \ln F}{\partial \ln \sqrt{\zeta}} = K(\mu) \qquad \text{with:} \quad \frac{\partial K}{\partial \ln \mu} = -\gamma_K(\alpha_s(\mu))$$

$$\frac{\partial \ln F}{\partial \ln \mu} = \gamma_F(\alpha_s(\mu)) - \gamma_K(\alpha_s(\mu)) \ln \frac{\sqrt{\zeta}}{\mu}$$

TMD structure

$$
\begin{aligned}
F_{f/P}(x, \mathbf{b}_T; \mu, \zeta) \quad &= \quad \sum_j C_{f/j}(x, b_*; \mu_b, \zeta_F) \otimes f_{j/P}(x, \mu_b) && : A \\
&\times \quad \exp\left\{ K(b_*; \mu_b) \ln \frac{\sqrt{\zeta_F}}{\mu_b} + \int_{\mu_b}^{\mu} \frac{d\mu'}{\mu'} \left[\gamma_F - \gamma_K \ln \frac{\sqrt{\zeta_F}}{\mu'} \right] \right\} && : B \\
&\times \quad \exp\left\{ g_{j/P}(x, b_T) + g_K(b_T) \ln \frac{\sqrt{\zeta_F}}{\sqrt{\zeta_{F,0}}} \right\} && : C
\end{aligned}
$$

TMD structure

$$F_{f/P}(x, \mathbf{b}_T; \mu, \zeta) = \sum_j C_{f/j}(x, b_*; \mu_b, \zeta_F) \otimes f_{j/P}(x, \mu_b) \qquad : A$$

$$\times \quad \exp\left\{ K(b_*; \mu_b) \ln \frac{\sqrt{\zeta_F}}{\mu_b} + \int_{\mu_b}^{\mu} \frac{d\mu'}{\mu'} \left[\gamma_F - \gamma_K \ln \frac{\sqrt{\zeta_F}}{\mu'} \right] \right\} \qquad : B$$

$$\times \quad \exp\left\{ g_{j/P}(x, b_T) + g_K(b_T) \ln \frac{\sqrt{\zeta_F}}{\sqrt{\zeta_{F,0}}} \right\} \qquad : C$$

- matching to collinear PDF at $b_T \ll 1/\Lambda_{QCD}$
- **perturbative**

TMD structure

$$F_{f/P}(x, \mathbf{b}_T; \mu, \zeta) = \sum_j C_{f/j}(x, b_*; \mu_b, \zeta_F) \otimes f_{j/P}(x, \mu_b) \qquad : A$$

$$\times \exp\left\{ K(b_*; \mu_b) \ln \frac{\sqrt{\zeta_F}}{\mu_b} + \int_{\mu_b}^{\mu} \frac{d\mu'}{\mu'} \left[\gamma_F - \gamma_K \ln \frac{\sqrt{\zeta_F}}{\mu'} \right] \right\} \qquad : B$$

$$\times \exp\left\{ g_{j/P}(x, b_T) + g_K(b_T) \ln \frac{\sqrt{\zeta_F}}{\sqrt{\zeta_{F,0}}} \right\} \qquad : C$$

- matching to collinear PDF at $b_T \ll 1/\Lambda_{QCD}$
- **perturbative**

- CS and RGE evolution to large b_T
- **perturbative**

Perturbative accuracy

Accuracy	H and C	K and γ_F	γ_K	PDF and α_s evolution
LL	0	-	1	-
NLL	0	1	2	LO
NLL’	1	1	2	NLO
NNLL	1	2	3	NLO
NNLL’	2	2	3	NNLO
N^3LL	2	3	4	NNLO

NLL $\quad C^0 \quad \alpha_S^n \ln^{2n}\left(\frac{Q^2}{\mu_b^2}\right), \quad \alpha_S^n \ln^{2n-1}\left(\frac{Q^2}{\mu_b^2}\right)$

NLL’ $\quad \left(C^0 + \alpha_S C^1\right) \quad \alpha_S^n \ln^{2n}\left(\frac{Q^2}{\mu_b^2}\right), \quad \alpha_S^n \ln^{2n-1}\left(\frac{Q^2}{\mu_b^2}\right)$

same logarithmic accuracy (difference = NNLL)

TMD structure

$$F_{f/P}(x, \mathbf{b}_T; \mu, \zeta) = \sum_j C_{f/j}(x, b_*; \mu_b, \zeta_F) \otimes f_{j/P}(x, \mu_b) \quad : A$$

$$\times \exp\left\{ K(b_*; \mu_b) \ln \frac{\sqrt{\zeta_F}}{\mu_b} + \int_{\mu_b}^{\mu} \frac{d\mu'}{\mu'} \left[\gamma_F - \gamma_K \ln \frac{\sqrt{\zeta_F}}{\mu'} \right] \right\} \quad : B$$

$$\times \exp\left\{ g_{j/P}(x, b_T) + g_K(b_T) \ln \frac{\sqrt{\zeta_F}}{\sqrt{\zeta_{F,0}}} \right\} \quad : C$$

- matching to collinear PDF at $b_T \ll 1/\Lambda_{QCD}$
- **perturbative**

$$\left(\mu_b = 2e^{-\gamma_E}/b_*\right)$$

- CS and RGE evolution to large b_T
- **perturbative**

- b_* prescription to avoid Landau pole

Non-perturbative: b* and f_{NP}

$$\alpha_s(\mu_b) = \alpha\left(\frac{2e^{-\gamma_E}}{b}\right) \gg 1 \quad \text{for large } b \text{ values}$$

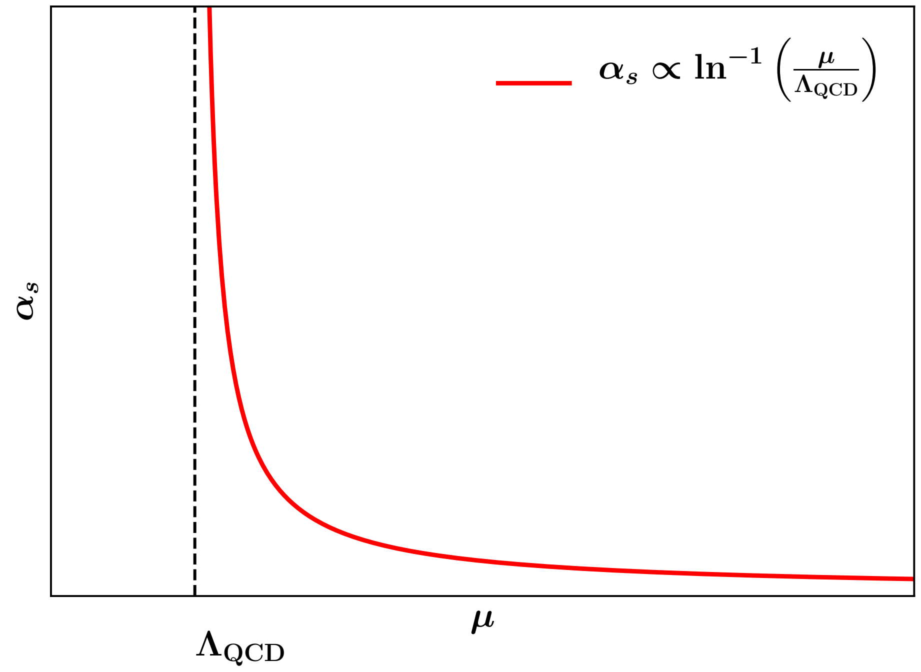

Non-perturbative: b* and f_{NP}

$$\alpha_s(\mu_b) = \alpha\left(\frac{2e^{-\gamma_E}}{b}\right) \gg 1 \quad \text{for large } b \text{ values}$$

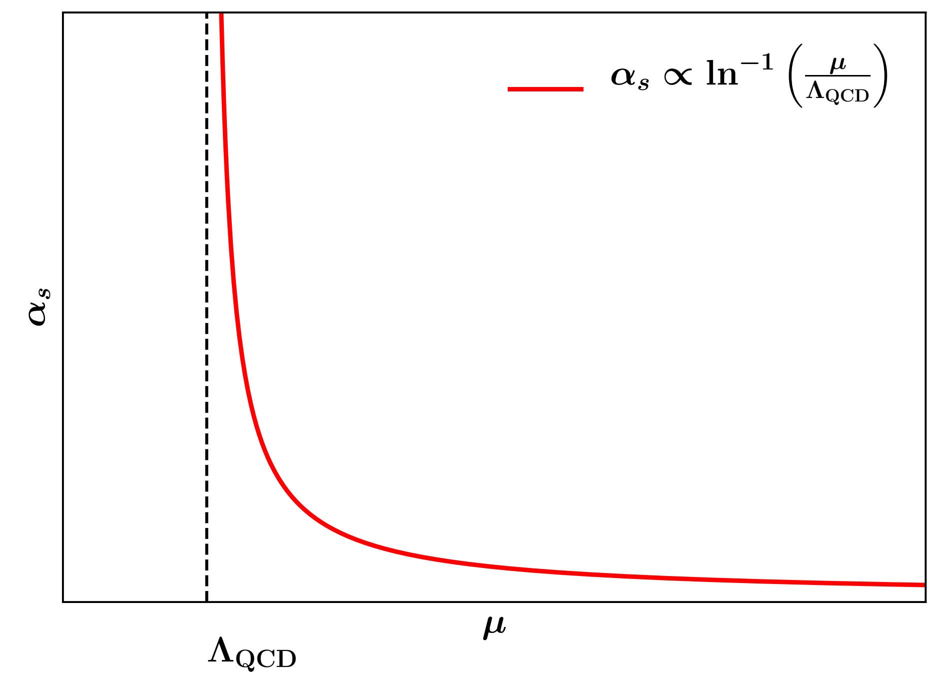

$$b_*(b) = b_{\rm max}\left(\frac{1-\exp\left(-\frac{b^4}{b_{\rm max}^4}\right)}{1-\exp\left(-\frac{b^4}{b_{\rm min}^4}\right)}\right)^{\frac{1}{4}}$$

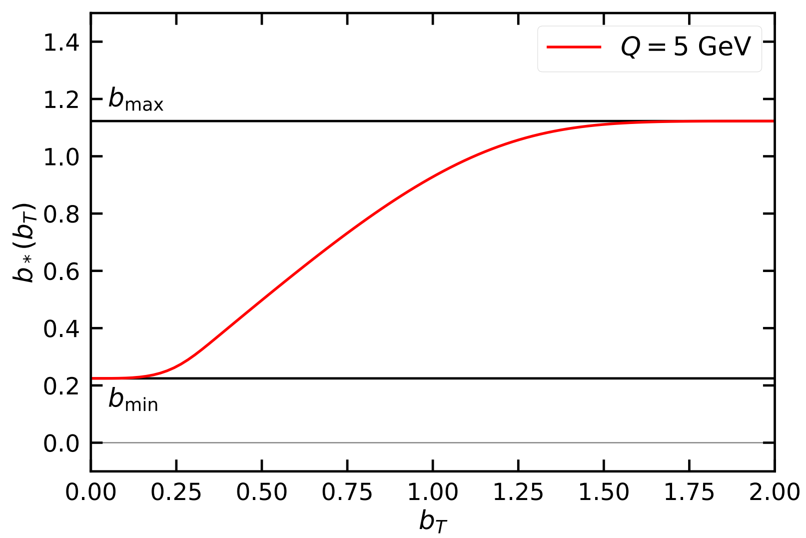

$$b_{\rm max} = 2e^{-\gamma_E}$$

$$b_{\rm min} = 2e^{-\gamma_E}/Q$$

TMD structure

$$F_{f/P}(x, \mathbf{b}_T; \mu, \zeta) = \sum_j C_{f/j}(x, b_*; \mu_b, \zeta_F) \otimes f_{j/P}(x, \mu_b) \quad : A$$

$$\times \exp\left\{ K(b_*; \mu_b) \ln \frac{\sqrt{\zeta_F}}{\mu_b} + \int_{\mu_b}^{\mu} \frac{d\mu'}{\mu'} \left[\gamma_F - \gamma_K \ln \frac{\sqrt{\zeta_F}}{\mu'} \right] \right\} \quad : B$$

$$\times \exp\left\{ g_{j/P}(x, b_T) + g_K(b_T) \ln \frac{\sqrt{\zeta_F}}{\sqrt{\zeta_{F,0}}} \right\} \quad f_{NP} \quad : C$$

$$\left(\mu_b = 2e^{-\gamma_E}/b_* \right)$$

- matching to collinear PDF at $b_T \ll 1/\Lambda_{QCD}$
- **perturbative**

- CS and RGE evolution to large b_T
- **perturbative**

- b_* prescription to avoid Landau pole
- f_{NP} "parametrises" the **non-perturbative** transverse modes
- **fit** f_{NP} to data

Non-perturbative: b* and f_{NP}

$$\alpha_s(\mu_b) = \alpha\left(\frac{2e^{-\gamma_E}}{b}\right) \gg 1 \quad \text{for large } b \text{ values}$$

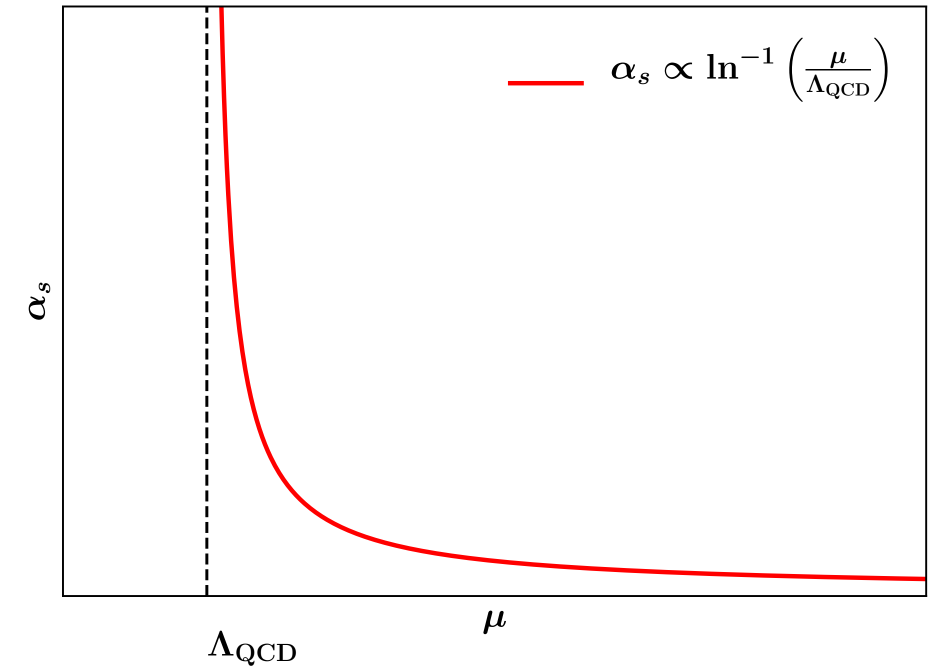

$$b_*(b) = b_{\max}\left(\frac{1-\exp\left(-\frac{b^4}{b_{\max}^4}\right)}{1-\exp\left(-\frac{b^4}{b_{\min}^4}\right)}\right)^{\frac{1}{4}}$$

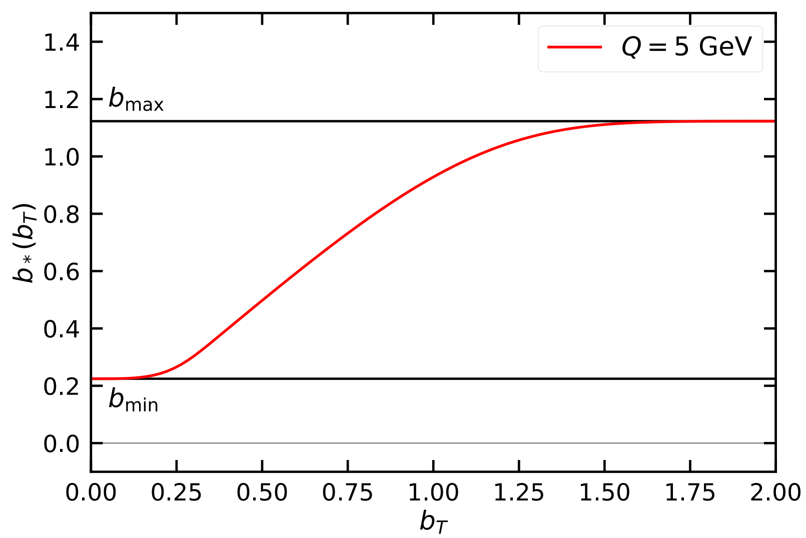

$$b_{\max} = 2e^{-\gamma_E}$$

$$b_{\min} = 2e^{-\gamma_E}/Q$$

f_{NP}

$$F(x,b;\mu,\zeta) = \left[\frac{F(x,b;\mu,\zeta)}{F(x,b_*(b);\mu,\zeta)}\right] F(x,b_*(b);\mu,\zeta)$$

- NP is unavoidable: intrinsically tied to regularisation procedure
- There is not a universal form factor:
  - depends on details of b* and collinear PDFs
  - requires definition of a functional form
  - determined through a fit to experimental data

The extraction of TMD PDFs and FFs from low-p_T data

DY data sets

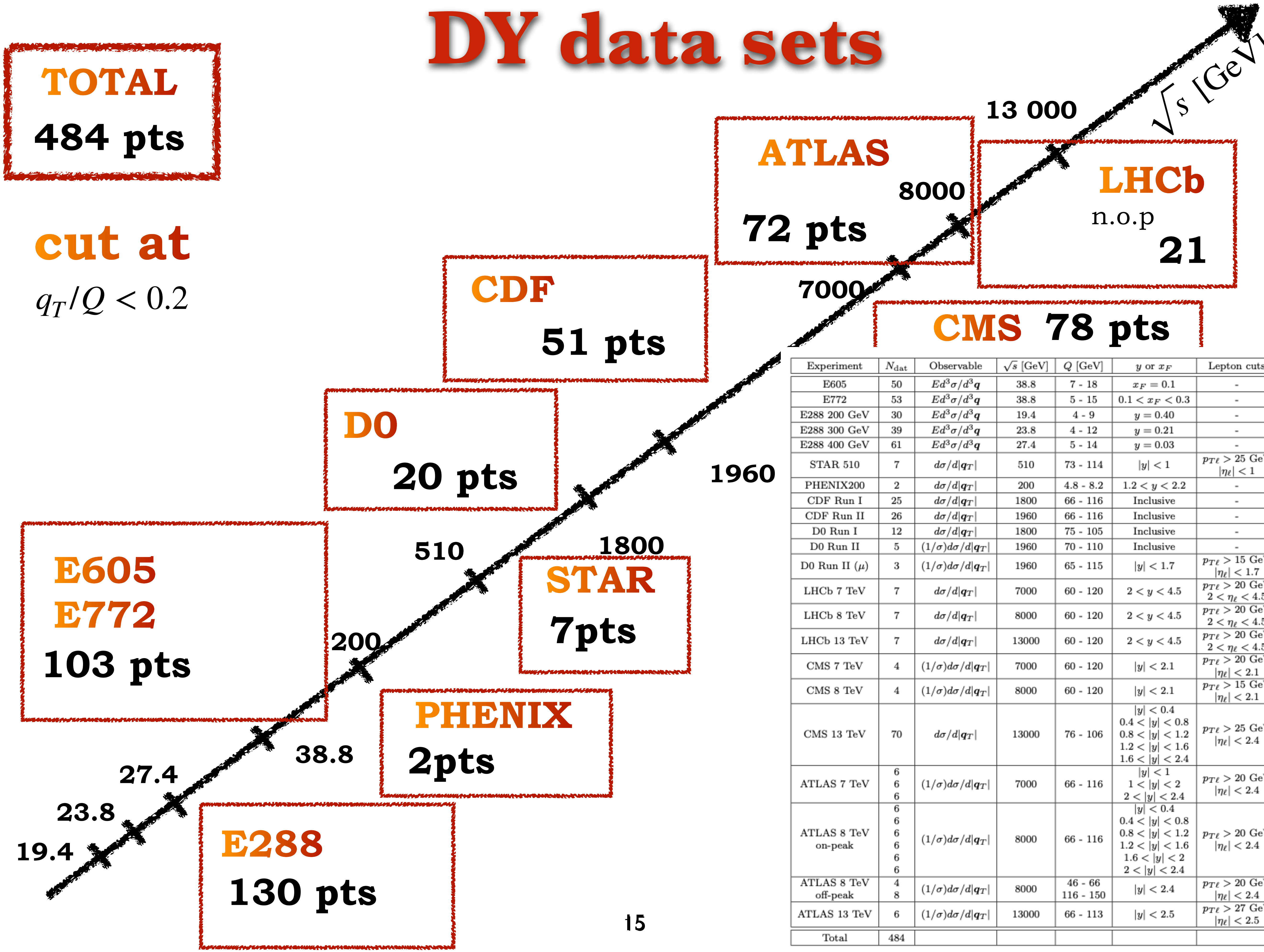

Experiment	N_{dat}	Observable	$\sqrt{s}$ [GeV]	Q [GeV]	y or x_F	Lepton cuts
E605	50	$Ed^3\sigma/d^3\boldsymbol{q}$	38.8	7 - 18	$x_F = 0.1$	-
E772	53	$Ed^3\sigma/d^3\boldsymbol{q}$	38.8	5 - 15	$0.1 < x_F < 0.3$	-
E288 200 GeV	30	$Ed^3\sigma/d^3\boldsymbol{q}$	19.4	4 - 9	$y = 0.40$	-
E288 300 GeV	39	$Ed^3\sigma/d^3\boldsymbol{q}$	23.8	4 - 12	$y = 0.21$	-
E288 400 GeV	61	$Ed^3\sigma/d^3\boldsymbol{q}$	27.4	5 - 14	$y = 0.03$	-
STAR 510	7	$d\sigma/d\lvert\boldsymbol{q}_T\rvert$	510	73 - 114	$\lvert y\rvert < 1$	$p_{T\ell} > 25$ GeV $\lvert\eta_\ell\rvert < 1$
PHENIX200	2	$d\sigma/d\lvert\boldsymbol{q}_T\rvert$	200	4.8 - 8.2	$1.2 < y < 2.2$	-
CDF Run I	25	$d\sigma/d\lvert\boldsymbol{q}_T\rvert$	1800	66 - 116	Inclusive	-
CDF Run II	26	$d\sigma/d\lvert\boldsymbol{q}_T\rvert$	1960	66 - 116	Inclusive	-
D0 Run I	12	$d\sigma/d\lvert\boldsymbol{q}_T\rvert$	1800	75 - 105	Inclusive	-
D0 Run II	5	$(1/\sigma)d\sigma/d\lvert\boldsymbol{q}_T\rvert$	1960	70 - 110	Inclusive	-
D0 Run II (μ)	3	$(1/\sigma)d\sigma/d\lvert\boldsymbol{q}_T\rvert$	1960	65 - 115	$\lvert y\rvert < 1.7$	$p_{T\ell} > 15$ GeV $\lvert\eta_\ell\rvert < 1.7$
LHCb 7 TeV	7	$d\sigma/d\lvert\boldsymbol{q}_T\rvert$	7000	60 - 120	$2 < y < 4.5$	$p_{T\ell} > 20$ GeV $2 < \eta_\ell < 4.5$
LHCb 8 TeV	7	$d\sigma/d\lvert\boldsymbol{q}_T\rvert$	8000	60 - 120	$2 < y < 4.5$	$p_{T\ell} > 20$ GeV $2 < \eta_\ell < 4.5$
LHCb 13 TeV	7	$d\sigma/d\lvert\boldsymbol{q}_T\rvert$	13000	60 - 120	$2 < y < 4.5$	$p_{T\ell} > 20$ GeV $2 < \eta_\ell < 4.5$
CMS 7 TeV	4	$(1/\sigma)d\sigma/d\lvert\boldsymbol{q}_T\rvert$	7000	60 - 120	$\lvert y\rvert < 2.1$	$p_{T\ell} > 20$ GeV $\lvert\eta_\ell\rvert < 2.1$
CMS 8 TeV	4	$(1/\sigma)d\sigma/d\lvert\boldsymbol{q}_T\rvert$	8000	60 - 120	$\lvert y\rvert < 2.1$	$p_{T\ell} > 15$ GeV $\lvert\eta_\ell\rvert < 2.1$
CMS 13 TeV	70	$d\sigma/d\lvert\boldsymbol{q}_T\rvert$	13000	76 - 106	$\lvert y\rvert < 0.4$ $0.4 < \lvert y\rvert < 0.8$ $0.8 < \lvert y\rvert < 1.2$ $1.2 < \lvert y\rvert < 1.6$ $1.6 < \lvert y\rvert < 2.4$	$p_{T\ell} > 25$ GeV $\lvert\eta_\ell\rvert < 2.4$
ATLAS 7 TeV	6 6 6	$(1/\sigma)d\sigma/d\lvert\boldsymbol{q}_T\rvert$	7000	66 - 116	$\lvert y\rvert < 1$ $1 < \lvert y\rvert < 2$ $2 < \lvert y\rvert < 2.4$	$p_{T\ell} > 20$ GeV $\lvert\eta_\ell\rvert < 2.4$
ATLAS 8 TeV on-peak	6 6 6 6 6 6	$(1/\sigma)d\sigma/d\lvert\boldsymbol{q}_T\rvert$	8000	66 - 116	$\lvert y\rvert < 0.4$ $0.4 < \lvert y\rvert < 0.8$ $0.8 < \lvert y\rvert < 1.2$ $1.2 < \lvert y\rvert < 1.6$ $1.6 < \lvert y\rvert < 2$ $2 < \lvert y\rvert < 2.4$	$p_{T\ell} > 20$ GeV $\lvert\eta_\ell\rvert < 2.4$
ATLAS 8 TeV off-peak	4 8	$(1/\sigma)d\sigma/d\lvert\boldsymbol{q}_T\rvert$	8000	46 - 66 116 - 150	$\lvert y\rvert < 2.4$	$p_{T\ell} > 20$ GeV $\lvert\eta_\ell\rvert < 2.4$
ATLAS 13 TeV	6	$(1/\sigma)d\sigma/d\lvert\boldsymbol{q}_T\rvert$	13000	66 - 113	$\lvert y\rvert < 2.5$	$p_{T\ell} > 27$ GeV $\lvert\eta_\ell\rvert < 2.5$
Total	484					

SIDIS data sets

Hermes

344 pts

Compass

1203 pts

TOTAL

1547 pts

1 4 15

$\sqrt{s}$ [GeV]

Experiment	N_{dat}	Observable	Channels	Q [GeV]	x	z	Phase space cuts
HERMES	344	$M(x, z, \|\boldsymbol{P}_{hT}\|, Q)$	$p \to \pi^+$ $p \to \pi^-$ $p \to K^+$ $p \to K^-$ $d \to \pi^+$ $d \to \pi^-$ $d \to K^+$ $d \to K^-$	1 - $\sqrt{15}$	$0.023 < x < 0.6$ (6 bins)	$0.1 < z < 1.1$ (8 bins)	$W^2 > 10$ GeV^2 $0.1 < y < 0.85$
COMPASS	1203	$M(x, z, \boldsymbol{P}_{hT}^2, Q)$	$d \to h^+$ $d \to h^-$	1 - 9 (5 bins)	$0.003 < x < 0.4$ (8 bins)	$0.2 < z < 0.8$ (4 bins)	$W^2 > 25$ GeV^2 $0.1 < y < 0.9$
Total	1547						

cut at

$Q > 1.4$ GeV
(coll. factorisation)

$0.2 < z < 0.7$
(no exclusive processes)

$$P_{hT}|_{max} = min[min[\,0.2Q,\ 0.5zQ\,] + 0.3\ \text{GeV},\ zQ\,]$$

$(q_T/Q < 0.2)$

(x, Q^2) coverage

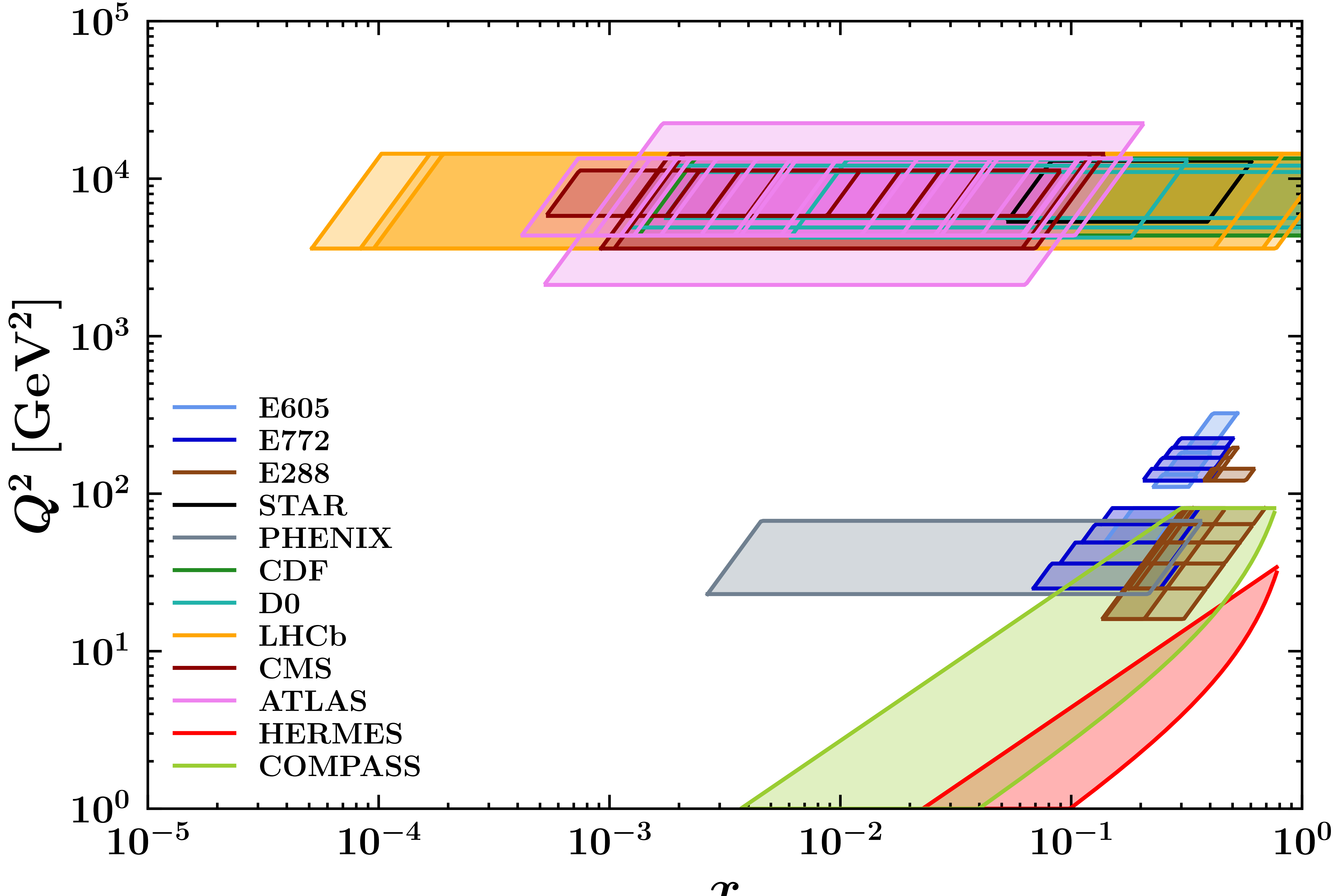

TMD global fits

	Accuracy	HERMES	COMPASS	DY fixed target	DY collider	N. of points	χ^2/N
Pavia 2017 arXiv:1703.10157	NLL	✔	✔	✔	✔	8059	1.55
SV 2019 arXiv:1912.06532	N3LL⁻	✔	✔	✔	✔	1039	1.06
MAP 2022 arXiv:2206.07598	N3LL⁻	✔	✔	✔	✔	2031	1.06
MAP 2024 arXiv:2405.13833	N3LL	✔	✔	✔	✔	2031	1.08

Global extractions: quick facts

PV17 (NLL)	SV19 (N3LL)	MAP22 (N3LL)	MAP24 (N3LL)
11 parameters	11 parameters	21 parameters	20(96) parameters
JHEP 06 (2017) 081	JHEP 06 (2020) 137	JHEP 10 (2022) 127	JHEP 08 (2024) 28

Functional forms

SV

$$f_{NP}(x,b) = \exp\left(-\frac{\lambda_1(1-x)+\lambda_2 x + x(1-x)\lambda_5}{\sqrt{1+\lambda_3 x^{\lambda_4}\boldsymbol{b}^2}}\boldsymbol{b}^2\right)$$

$$\mathcal{D}(\mu,b) = \mathcal{D}_{\text{resum}}(\mu, b^*(b)) + c_0 b b^*(b),$$

$$b^*(b) = \frac{b}{\sqrt{1+\boldsymbol{b}^2/B_{\text{NP}}^2}}.$$

MAP

$$f_{1\text{NP}}(x, b_T^2) \propto \text{F.T. of } \left(e^{-\frac{k_\perp^2}{g_{1A}}} + \lambda_B k_\perp^2 e^{-\frac{k_\perp^2}{g_{1B}}} + \lambda_C e^{-\frac{k_\perp^2}{g_{1C}}}\right)$$

$$g_1(x) = N_1 \frac{(1-x)^\alpha\, x^\sigma}{(1-\hat{x})^\alpha\, \hat{x}^\sigma}$$

Collins-Soper kernel

$$f_{NP}(x, b_T^2)\exp\left\{g_K(b_T^2)\ln\frac{\sqrt{\zeta}}{\sqrt{\zeta_0}}\right\}$$

$$g_K(b_T^2) = -g_2^2\frac{b_T^2}{4}$$

Fit quality: SIDIS

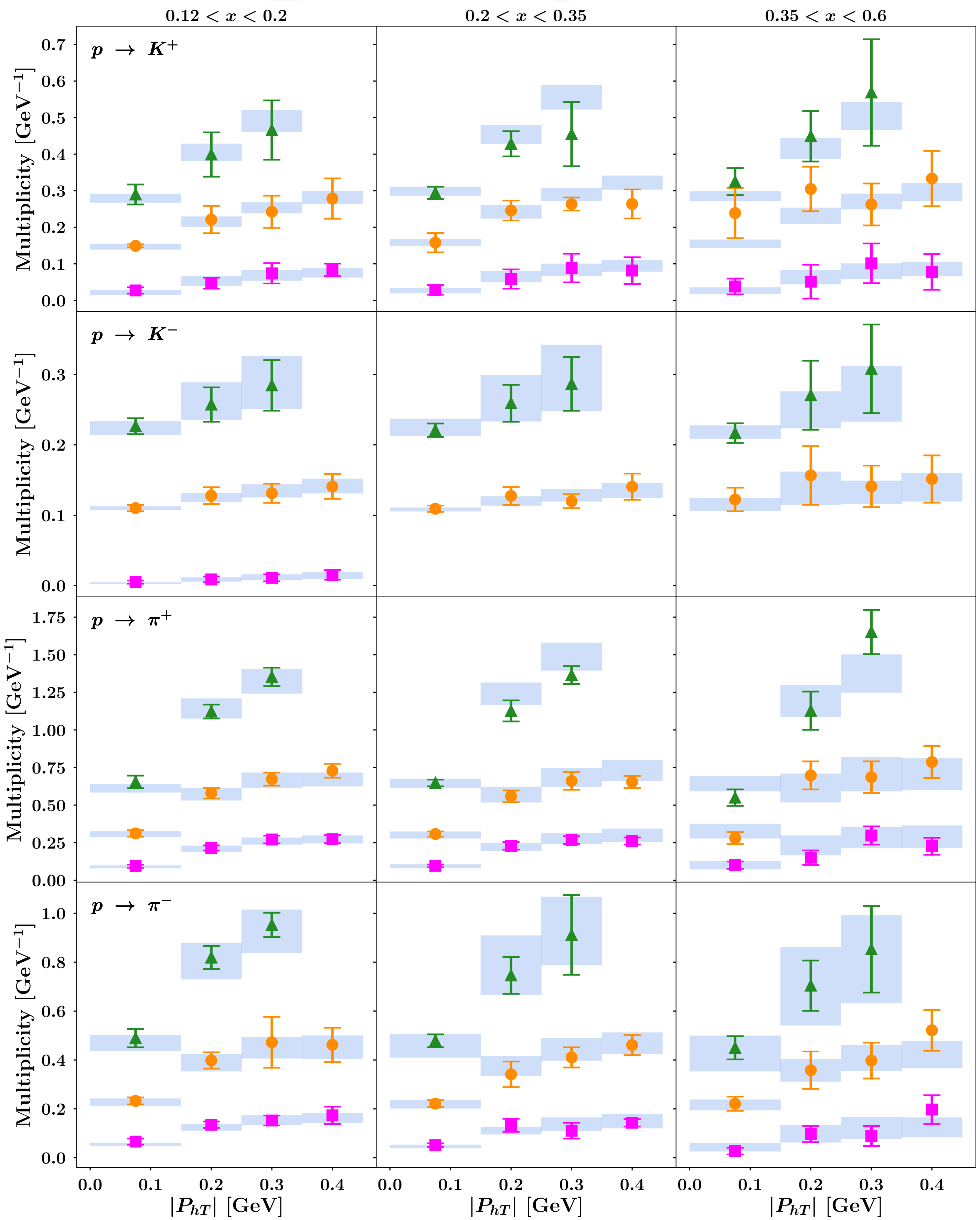

HERMES

Fit quality: Drell-Yan

E288

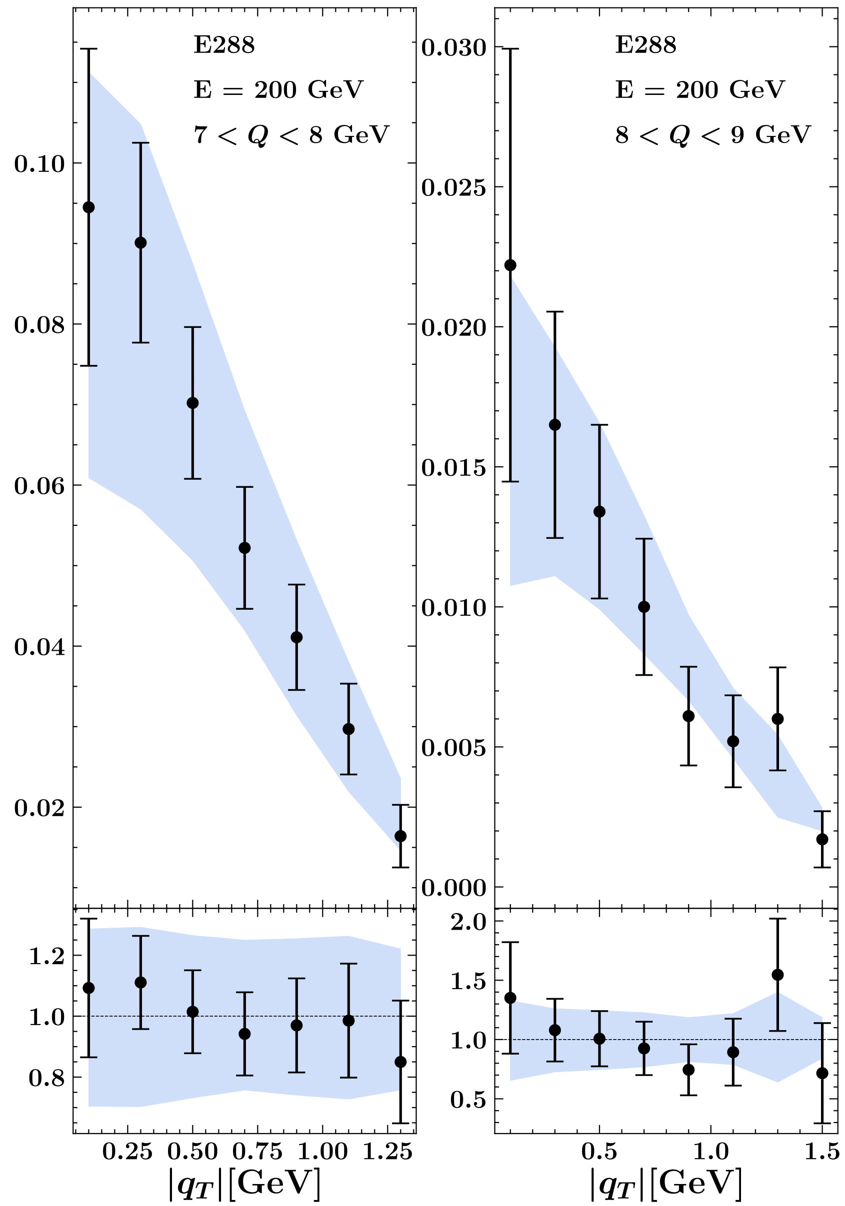

CMS

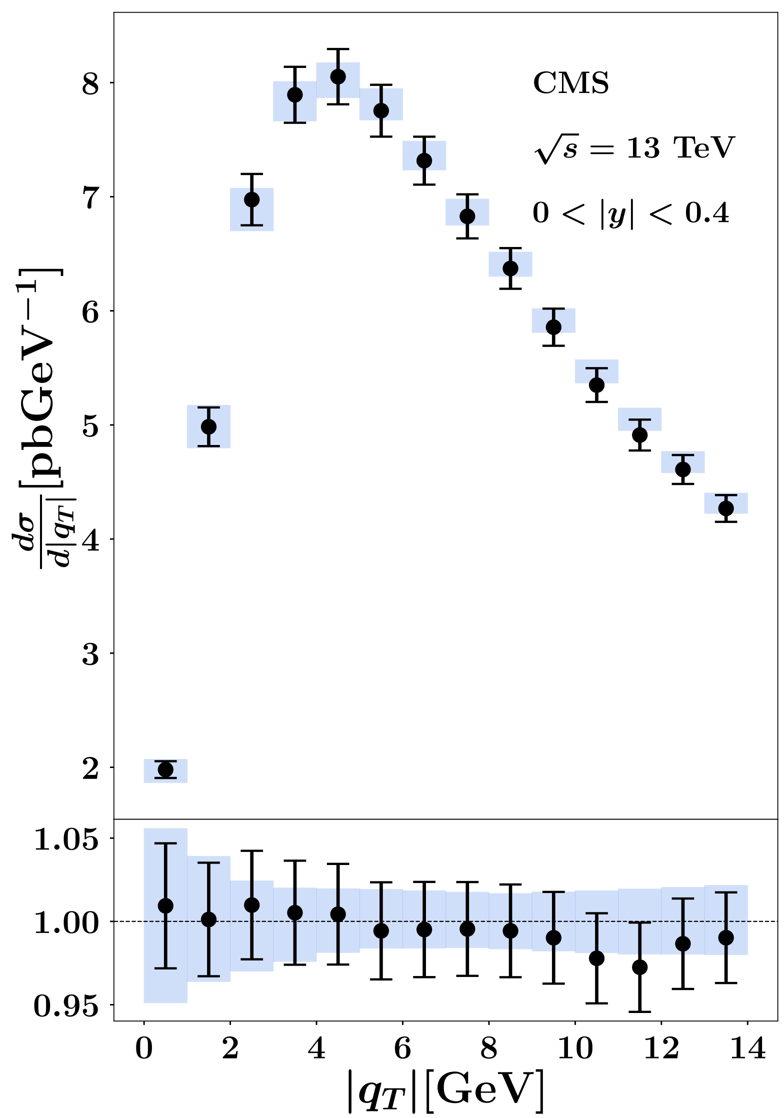

CDF

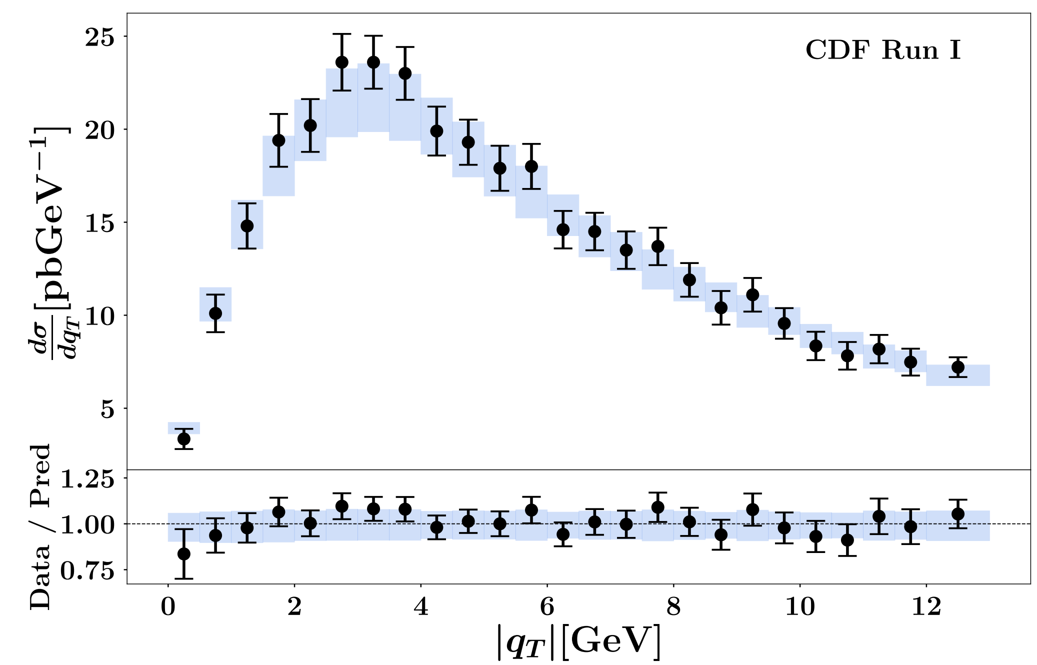

ATLAS

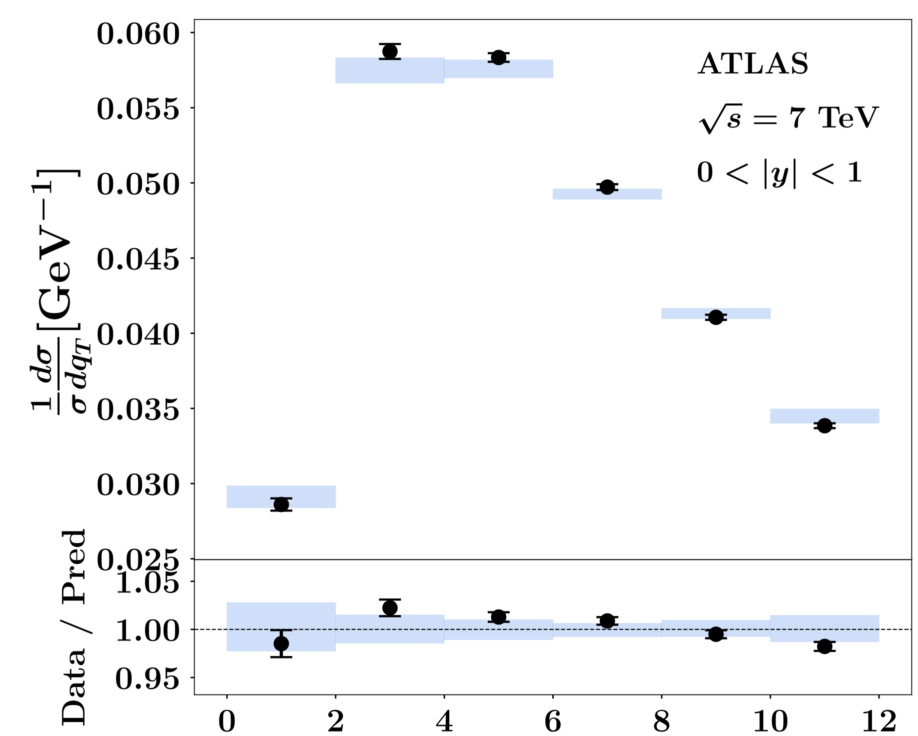

TMD PDFs

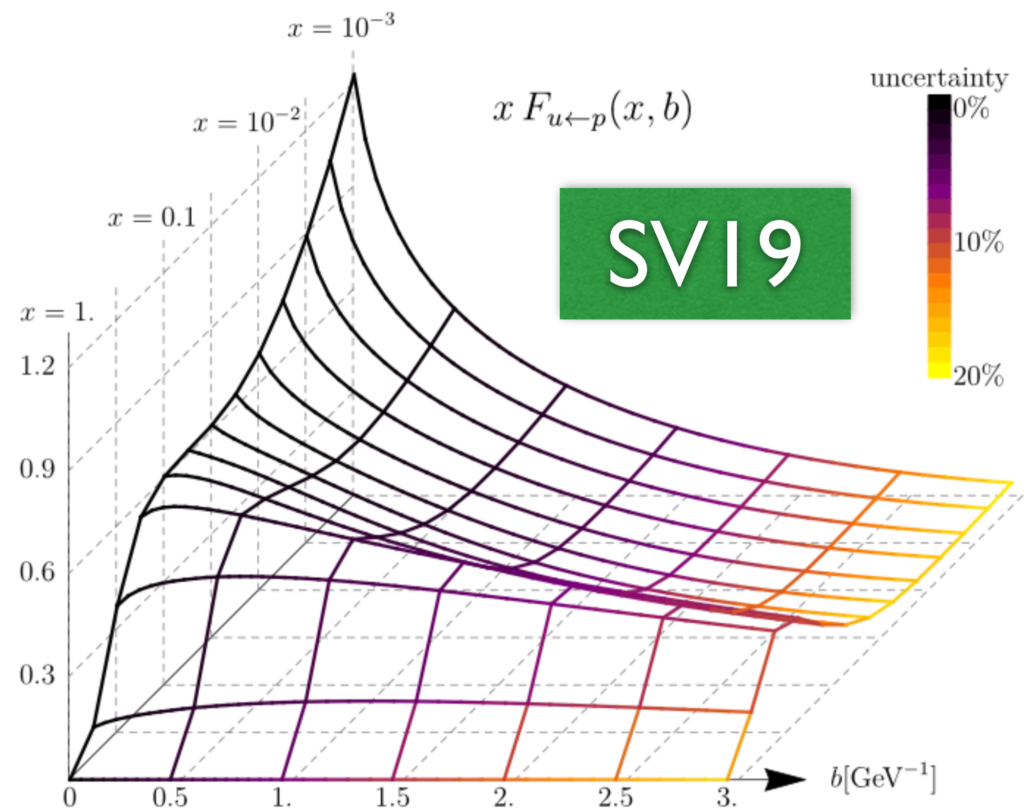

SV19
$x\,F_{u\leftarrow p}(x,b)$
$x=10^{-3}$
$x=10^{-2}$
$x=0.1$
$x=1.$
uncertainty
0%
10%
20%
1.2
0.9
0.6
0.3
0
0.5
1.
1.5
2.
2.5
3.
$b[\mathrm{GeV}^{-1}]$

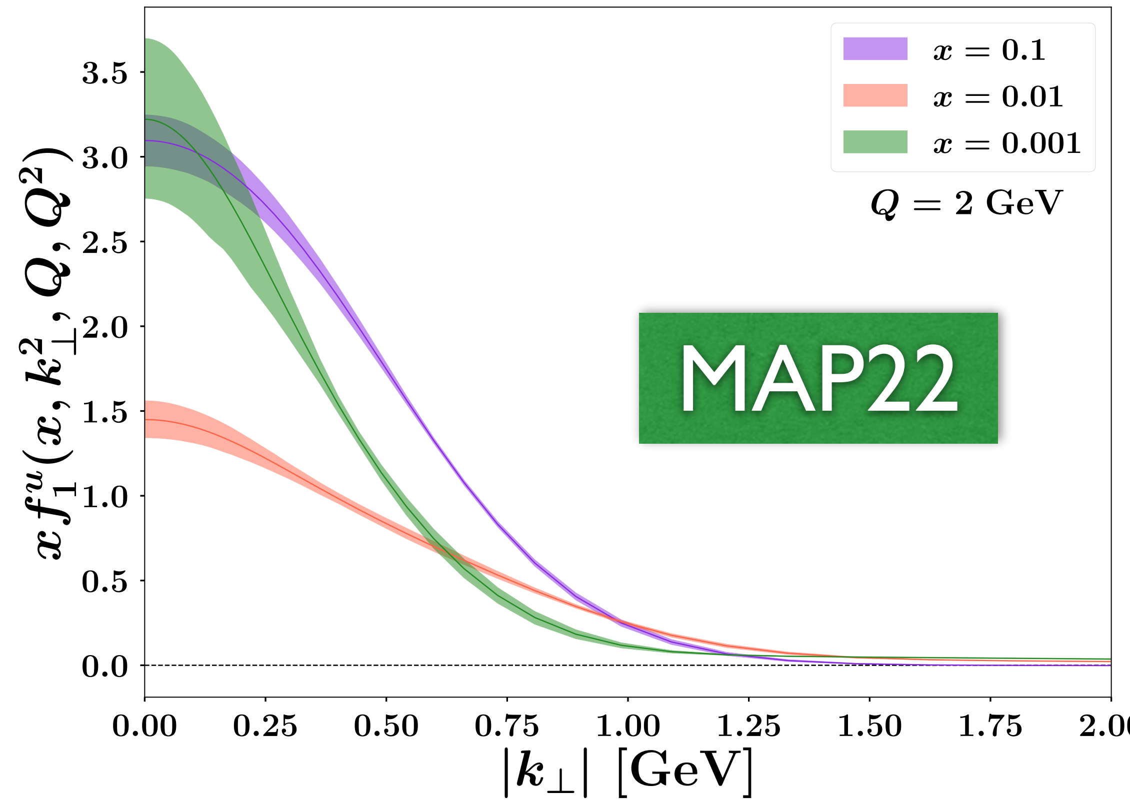

MAP22
$x = 0.1$
$x = 0.01$
$x = 0.001$
$Q = 2$ GeV
$x f_1^u(x, k_\perp^2, Q, Q^2)$
$|k_\perp|$ [GeV]
0.0
0.5
1.0
1.5
2.0
2.5
3.0
3.5
0.00
0.25
0.50
0.75
1.00
1.25
1.50
1.75
2.00

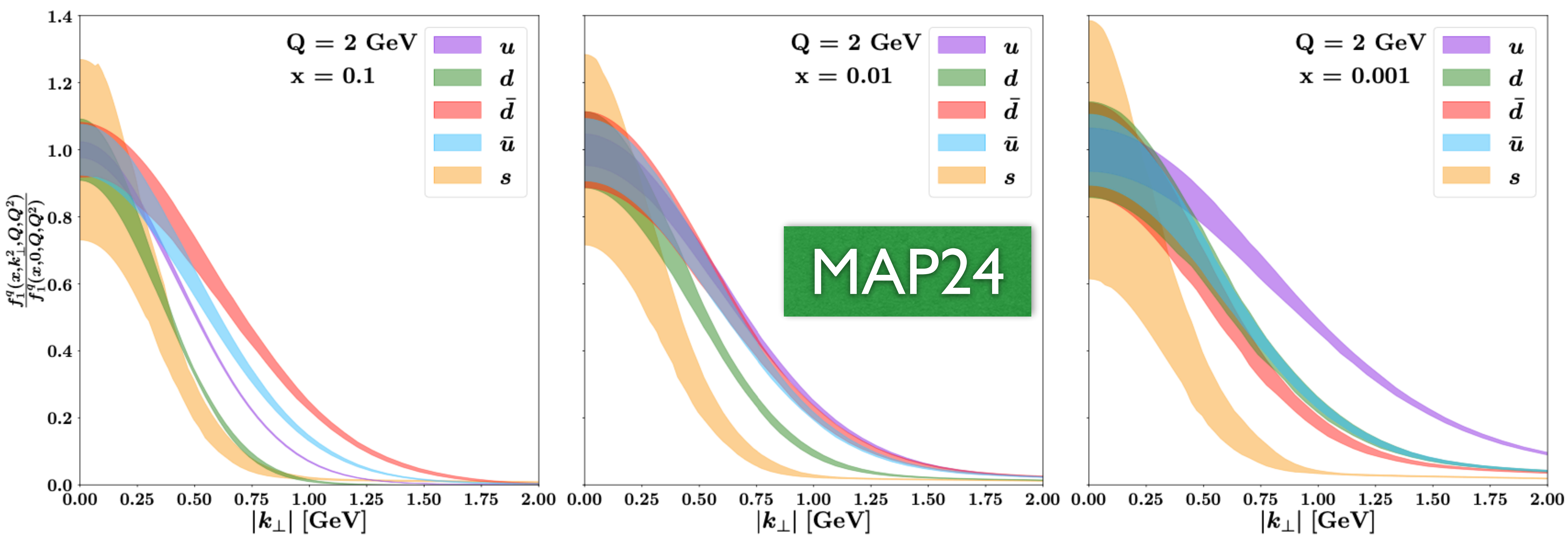

MAP24
Q = 2 GeV
x = 0.1
x = 0.01
x = 0.001
u
d
$\bar{d}$
$\bar{u}$
s
$\frac{f_1^q(x,k_\perp^2,Q,Q^2)}{f_1^q(x,0,Q,Q^2)}$
$|k_\perp|$ [GeV]
0.0
0.2
0.4
0.6
0.8
1.0
1.2
1.4
0.00
0.25
0.50
0.75
1.00
1.25
1.50
1.75
2.00

Collins-Soper kernel

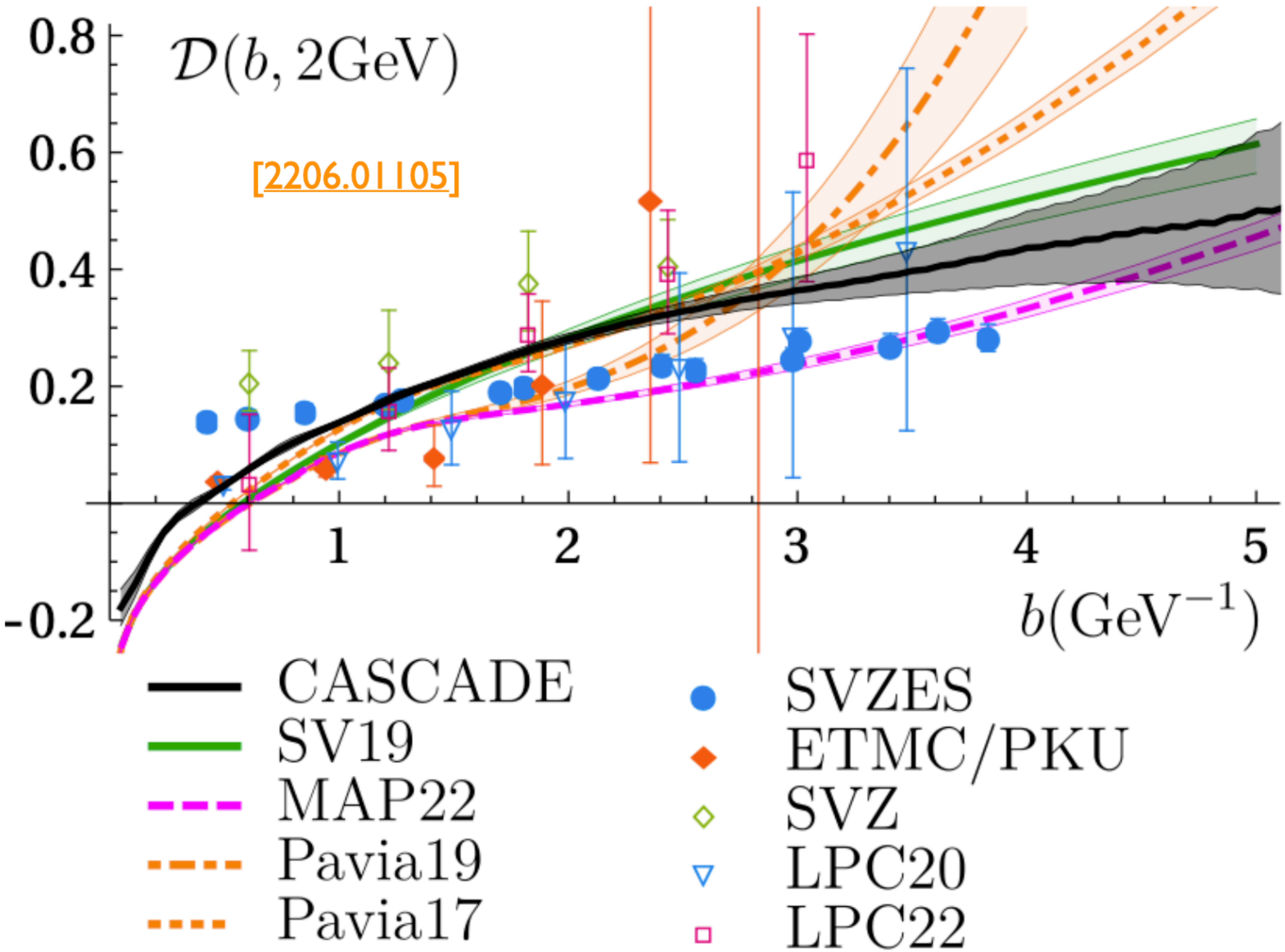

Perturbative convergence

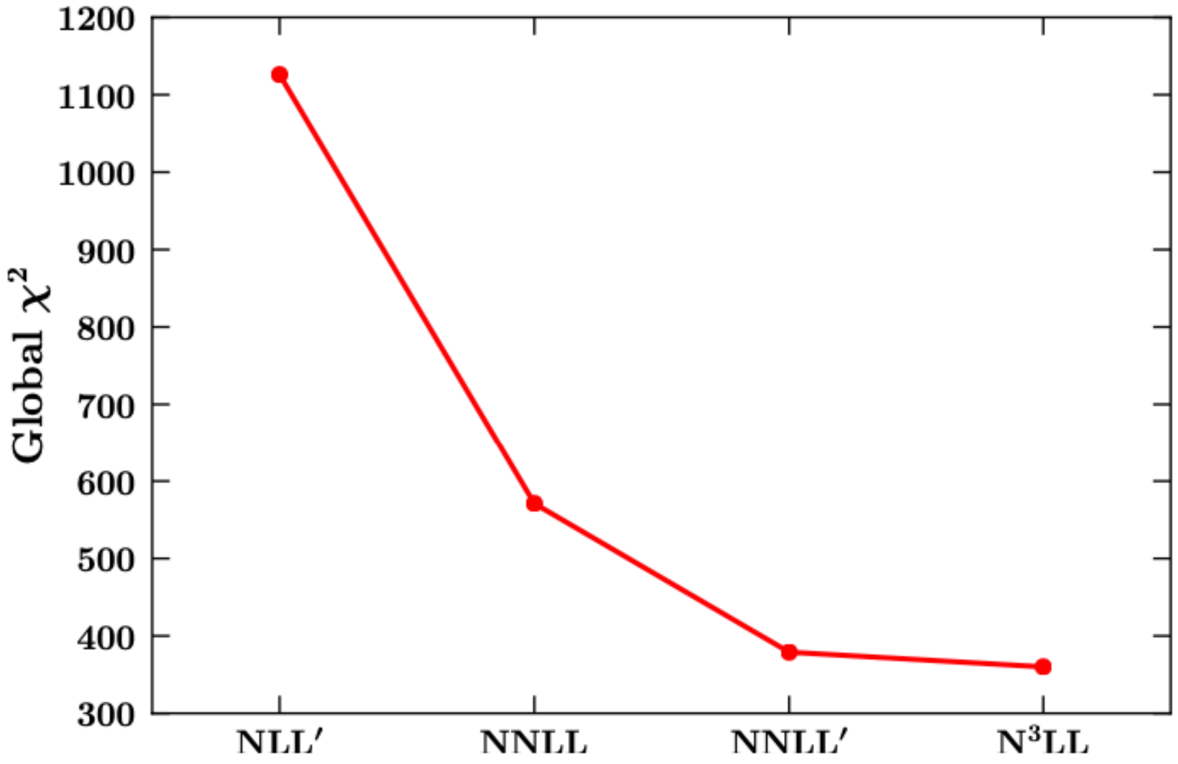

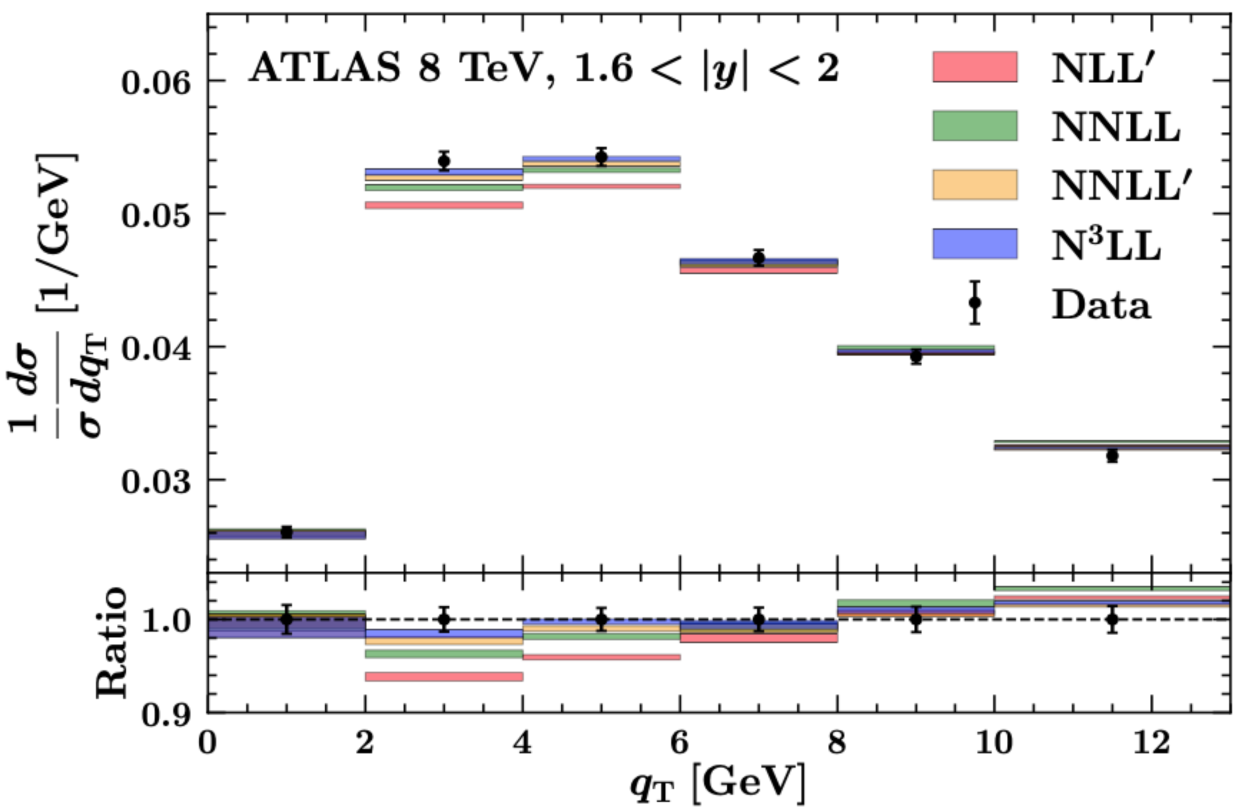

Order	NLL’	NNLL	NNLL’	N³LL
χ^2 /d.o.f.	3.19	1.62	1.07	**1.02**

(PV19) JHEP 07 (2020) 117

Importance of x-dependence

Test: *x*-independent fit at N³LL with Davies, Webber, Stirling (1985) NP parameterisation:

$$f_{NP}^{DWS}(b_T,\zeta) = \exp\left[-\frac{1}{2}\left(g_1 + g_2 \ln\left(\frac{\zeta}{2Q_0^2}\right)\right) b_T^2\right]$$

with and without ATLAS data

	Full dataset	No y-differential data
Global χ^2/N_{dat}	1.339	0.895
g_1	0.304	0.207
g_2	0.028	0.093

- χ^2 significantly higher for full dataset (1.339 vs. 1.020)
  - x-dependence required to describe data
- χ^2 significantly lower without ATLAS data
  - x-dependence at N³LL driven by ATLAS data

(PV19) JHEP 07 (2020) 117

Relevance of f_{NP} at high Q

- N^3LL fit to DY data only with $f_{NP} = 1$ or MAP 22
- different values of $[q_T/Q]_{min}$

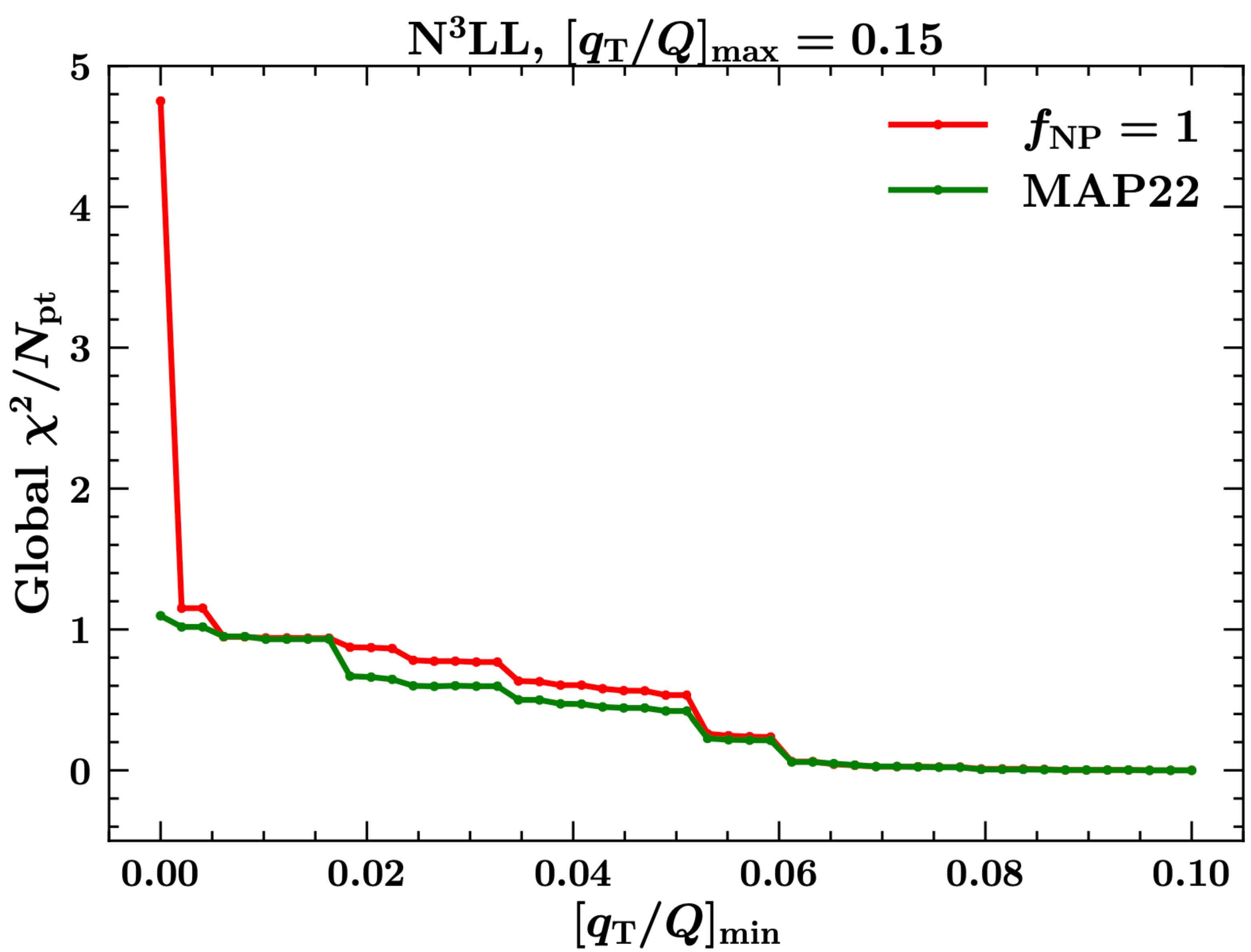

Relevance of f_{NP} at high Q

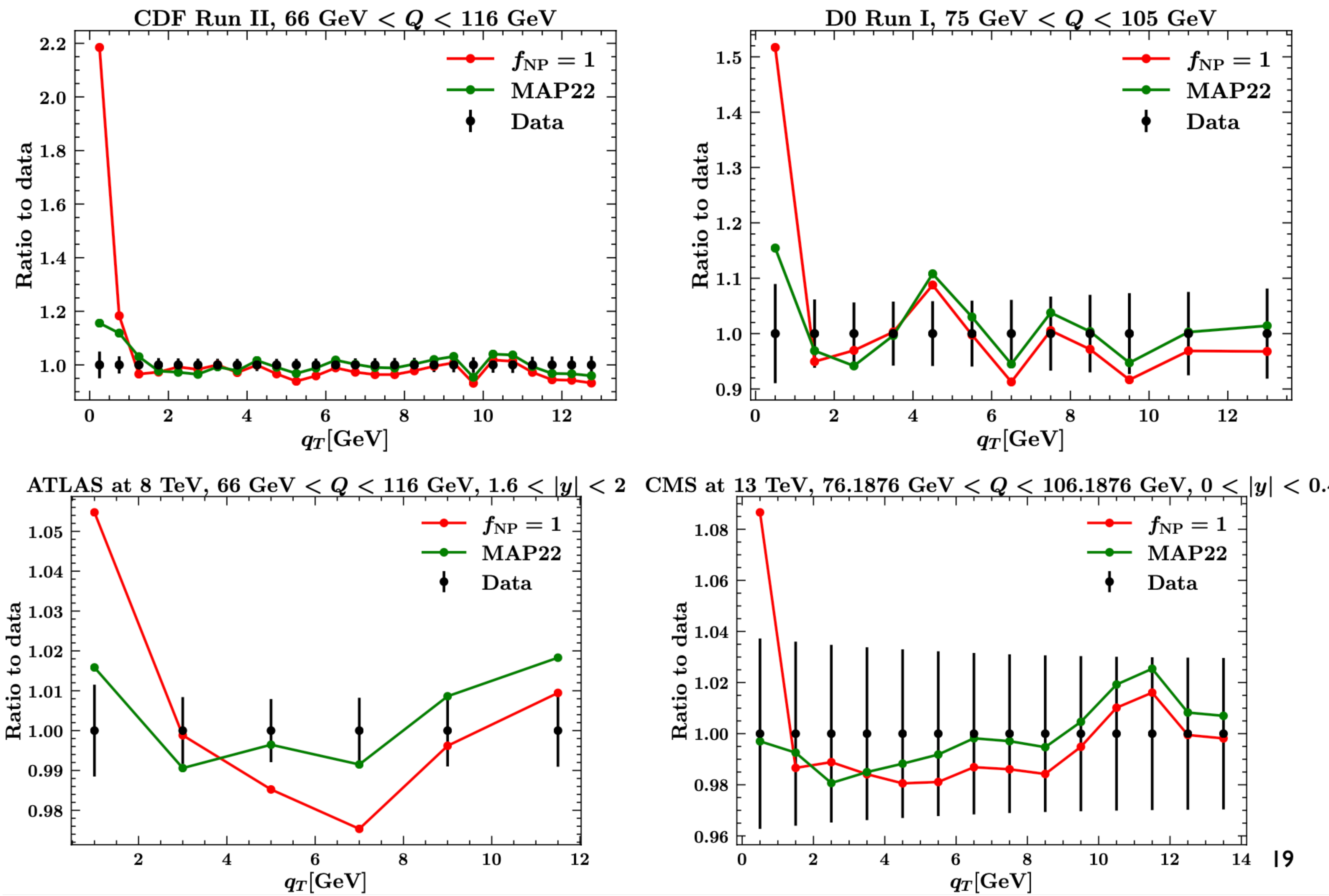

Future: matching with F.O.

- **Matching** between TMD and collinear factorisations:

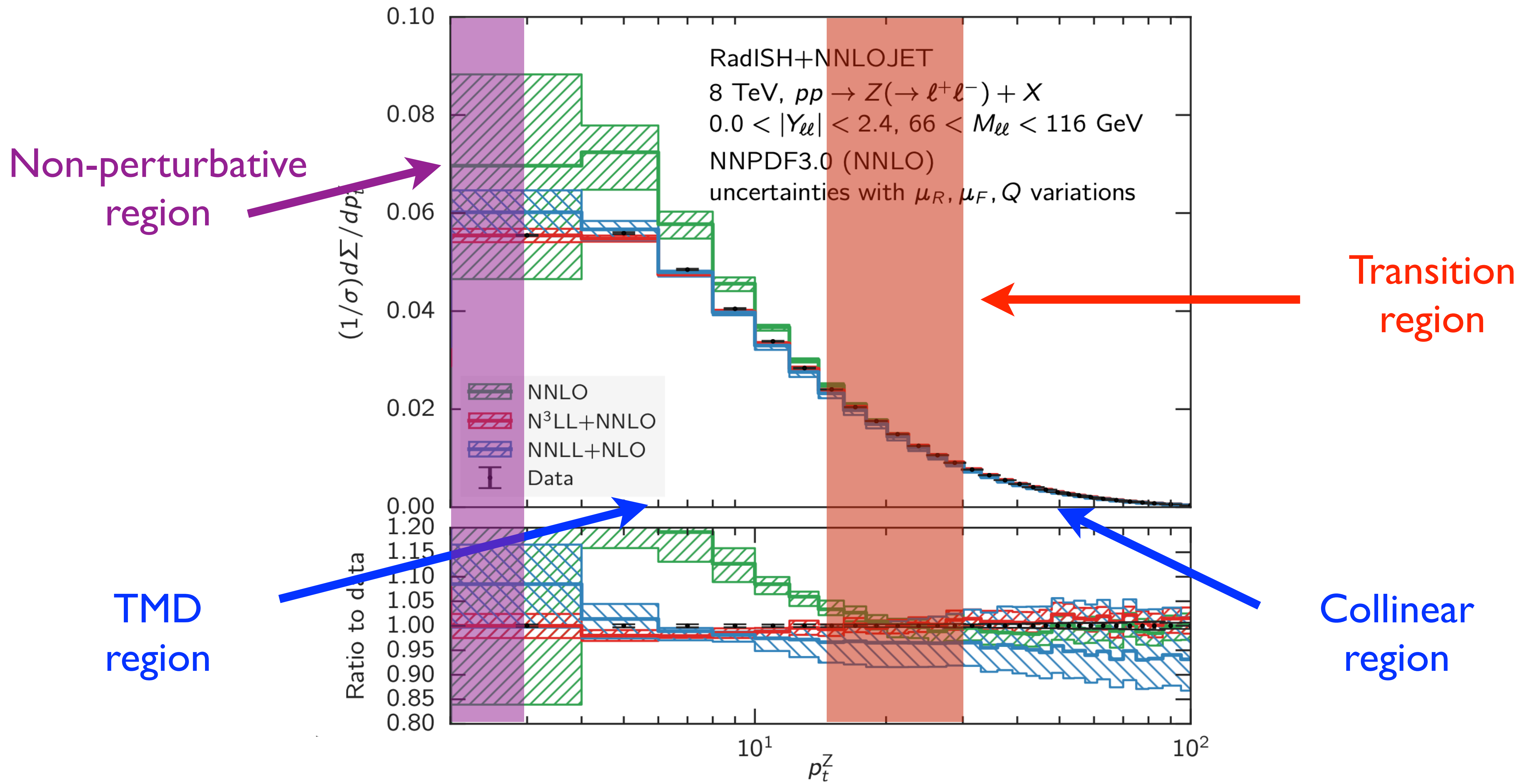

- Well-understood procedure at the LHC energies where usually $Q \gg \Lambda_{\rm QCD}$:
  - clear separation of TMD and collinear, non-perturbative confined to very low q_T.
- Not so much so for current (and future) SIDIS data due to smaller Q:
  - need to *identify* and *study* the transition region.

Future: Exp. Measurements

- TMD factorisation applies for $q_T \ll Q$:
  - the region $q_T \simeq \Lambda_{QCD}$ is relevant for hadron structure, no matter how large Q.
  - As Q increases the cross section drops and low q_T becomes hard to access.

Need as many (low-q_T + y-binned) data as possible!

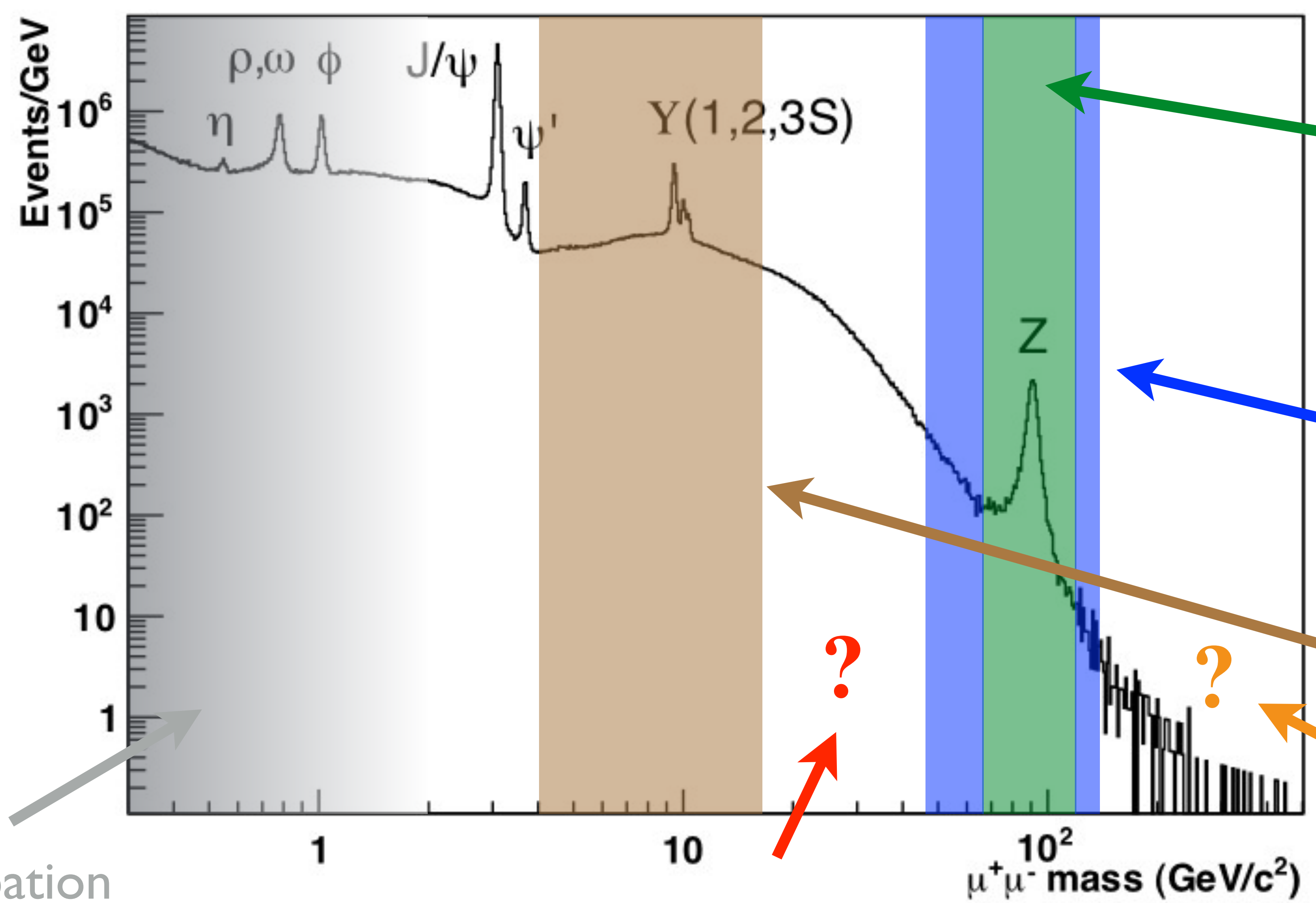

Future: Exp. Measurements

$$\phi^*_\eta = \tan\left(\frac{\pi - \Delta\phi_\ell}{2}\right)\sqrt{1 - \tanh^2\left(\frac{\Delta\eta_\ell}{2}\right)}$$

[Banfi et *al.*, 1009.1580]

- Small ϕ^* is mapped onto small q_T, this observable is expected to carry important information on hadron structure.

- Experimentally very clean because it only involves angles.
  - Only angles: insanely precise!
  - $\phi^*_\eta \approx \dfrac{q_T}{M}$
  - definitely relevant for hadron structure
  - it might be interesting to check shape variation with rapidity and m_{ll} at low ϕ^*_η(TMD (x, Q^2)-dependence)

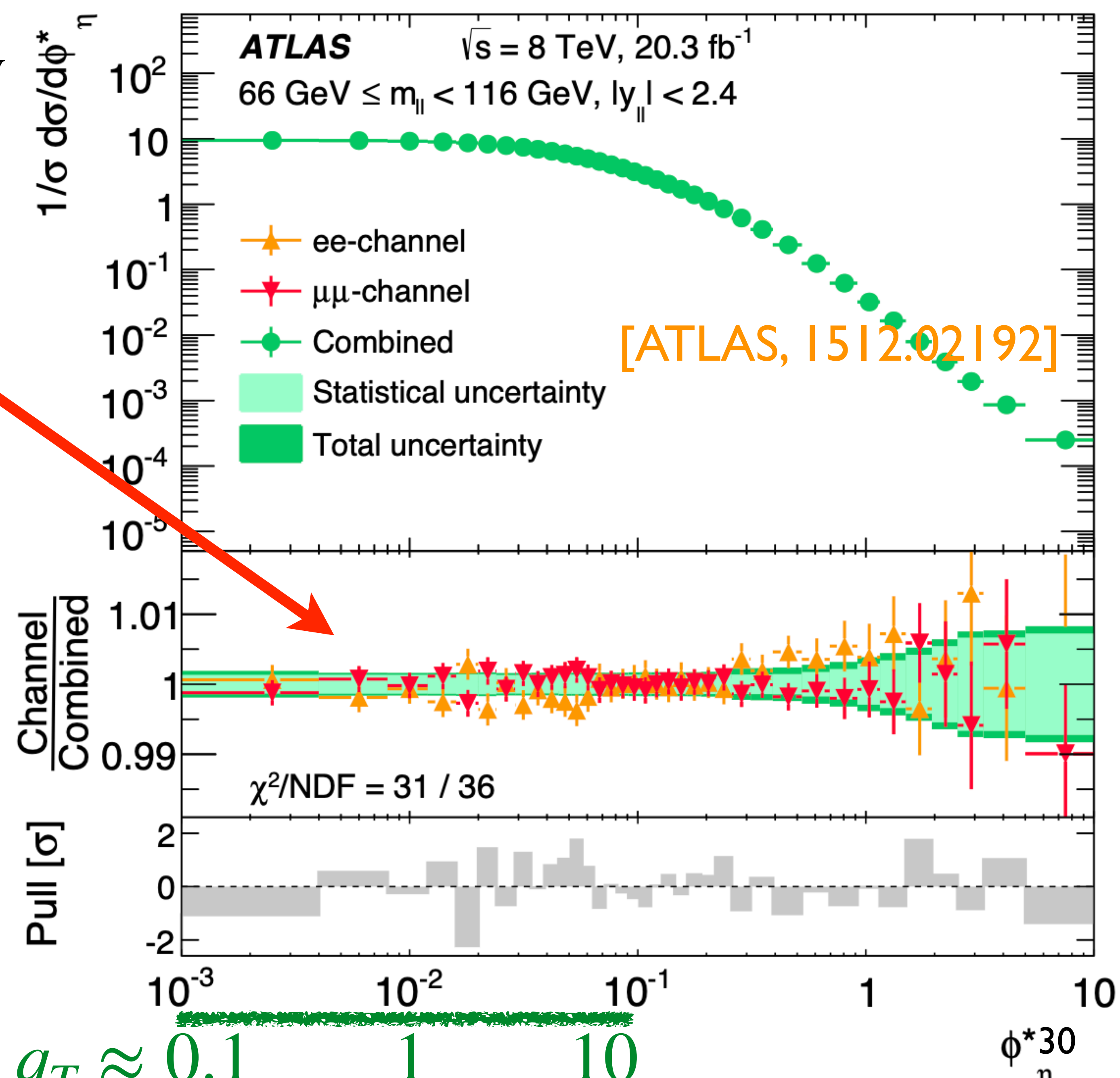

$q_T \approx 0.1 \quad 1 \quad 10$

Future: W mass measurements

- $p_{Tl} \leftarrow q_{TW} \leftarrow$ resummation + intrinsic-k_T
- <u>All analyses assume flavour-independence</u>
- <u>impact of flavour-dependent intrinsic-k_T comparable to PDF variations</u>

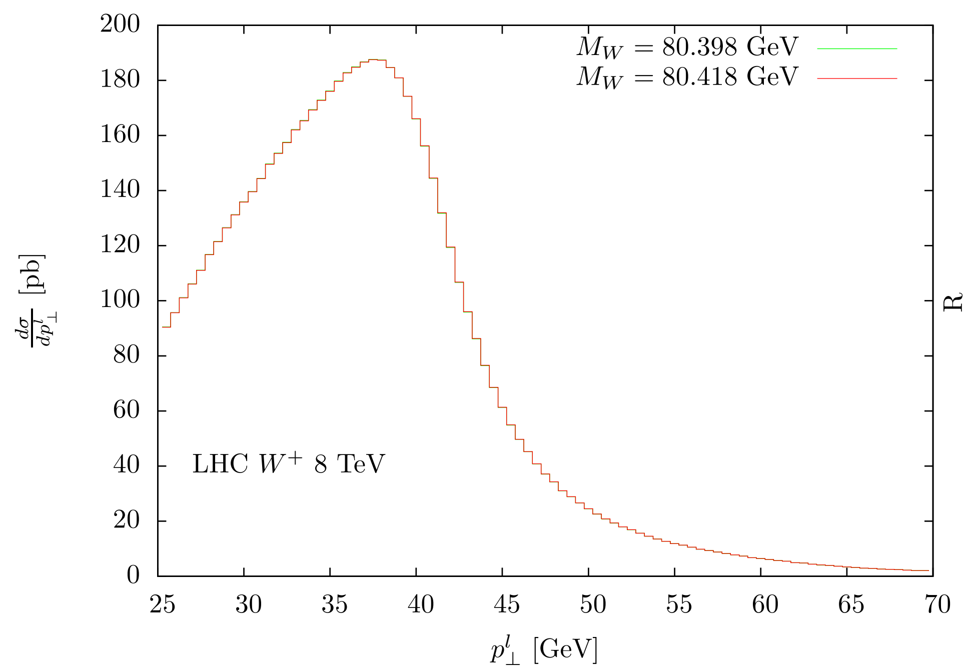

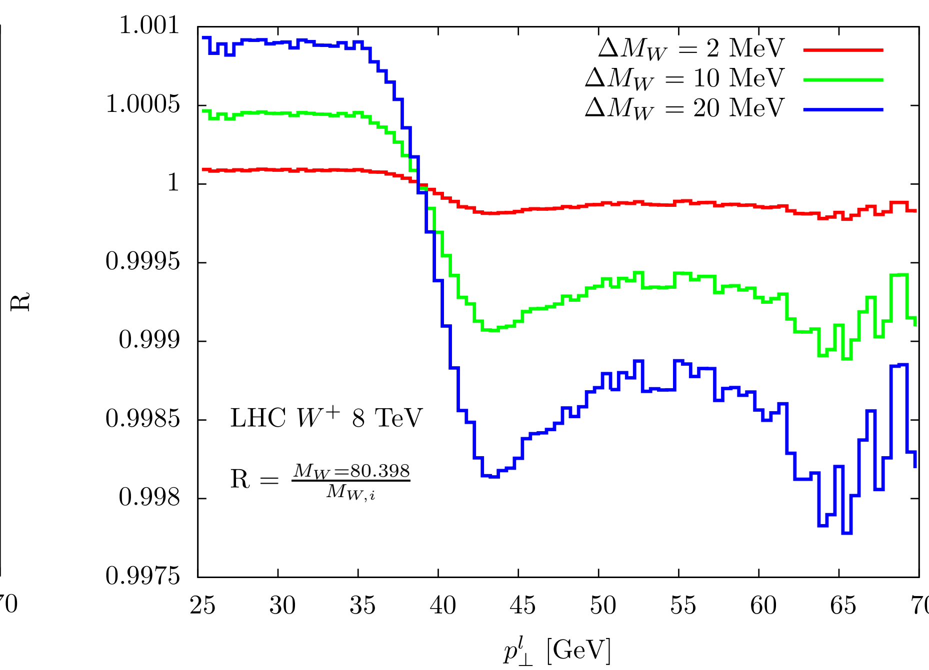

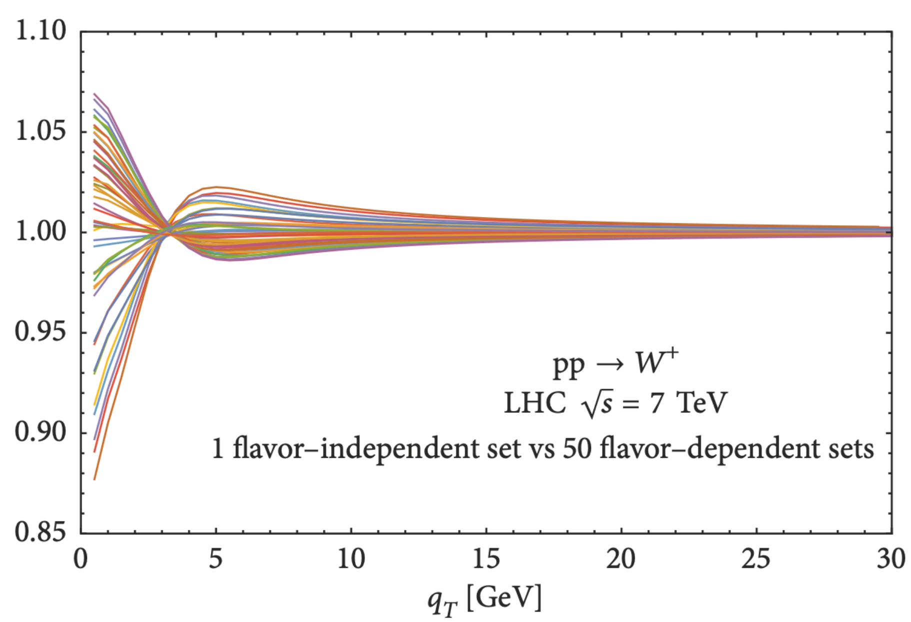

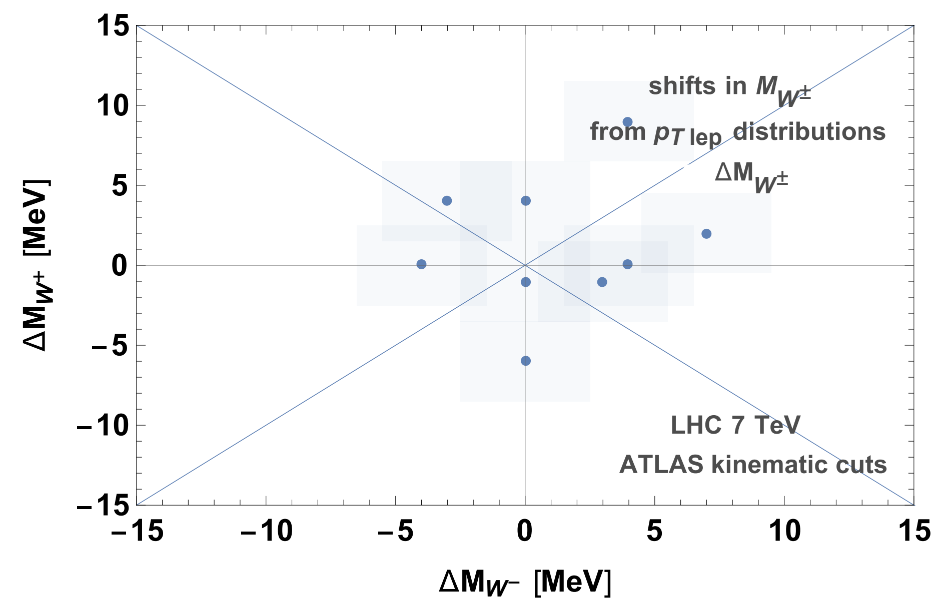

Thank you!